RANDOMIZED SINGLE-VIEW ALGORITHMS FOR LOW-RANK MATRIX APPROXIMATION*

JOEL A. TROPP†, ALP YURTSEVER‡, MADELEINE UDELL§, AND VOLKAN CEVHER¶

Abstract. This paper develops a suite of algorithms for constructing low-rank approximations of an input matrix from a random linear image of the matrix, called a *sketch*. These methods can preserve structural properties of the input matrix, such as positive-semidefiniteness, and they can produce approximations with a user-specified rank. The algorithms are simple, accurate, numerically stable, and provably correct. Moreover, each method is accompanied by an informative error bound that allows users to select parameters *a priori* to achieve a given approximation quality. These claims are supported by computer experiments.

Key words. Dimension reduction; matrix approximation; numerical linear algebra; randomized algorithm; single-pass algorithm; single-view algorithm; streaming algorithm; subspace embedding.

AMS subject classifications. Primary, 65F30; Secondary, 68W20.

1. Motivation.

This paper develops a framework for computing structured low-rank approximations of a matrix from a (random) linear image with lower dimension than the matrix itself. These techniques have applications in large-scale numerical linear algebra [14, 16, 25] and optimization [6], *inter alia*.

1.1. Low-Rank Matrix Approximation.

We work over the field $\mathbb{F} = \mathbb{R}$ or $\mathbb{F} = \mathbb{C}$. Suppose that $\boldsymbol{A} \in \mathbb{F}^{m\times n}$ is an arbitrary matrix. Let r be a target rank parameter where $r \ll \min\{m, n\}$. Our computational goal is to produce a low-rank reconstruction $\hat{\boldsymbol{A}}$ of the matrix $\boldsymbol{A}$ whose error is comparable with a best rank-r approximation:

$$\|\boldsymbol{A} - \hat{\boldsymbol{A}}\|_{\mathrm{F}} \approx \min_{\operatorname{rank} \boldsymbol{Z} \le r} \|\boldsymbol{A} - \boldsymbol{Z}\|_{\mathrm{F}}. \tag{1.1}$$

The notation $\|\cdot\|_{\mathrm{F}}$ refers to the Frobenius norm. We explicitly allow the rank of the approximation $\hat{\boldsymbol{A}}$ to be somewhat larger than r because it is easier to obtain an accurate approximation of this form. There has been extensive research on randomized algorithms for this problem; see the comprehensive treatment in Halko et al. [14].

1.2. Sketching.

Here is the twist. Imagine that our interactions with the matrix $\boldsymbol{A}$ are severely constrained in the following way. We are permitted to select a linear map $\mathcal{L} : \mathbb{F}^{m\times n} \to \mathbb{F}^d$ without reference to the matrix $\boldsymbol{A}$. Our only mechanism for collecting data S about $\boldsymbol{A}$ is to apply the linear map $\mathcal{L}$:

$$\mathsf{S} := \mathcal{L}(\boldsymbol{A}) \in \mathbb{F}^d. \tag{1.2}$$

We refer to S as a *sketch* of the matrix, and $\mathcal{L}$ is called a *sketching map*. The number d is called the *dimension* or *size* of the sketch.

---

*Date: 30 August 2016.

Funding: JAT and MU were supported in part by ONR Award N00014-11-1002 and the Gordon & Betty Moore Foundation. AY and VC were supported in part by the European Commission under Grant ERC Future Proof, SNF 200021-146750, and SNF CRSII2-147633.

†California Institute of Technology, Pasadena, CA (jtropp@cms.caltech.edu).

‡École Polytechnique Fédéral de Lausanne, Lausanne, Switzerland (alp.yurtsever@epfl.ch).

§Cornell University, Ithaca, NY (mru8@cornell.edu).

¶École Polytechnique Fédéral de Lausanne, Lausanne, Switzerland (volkan.cevher@epfl.ch).

The dimension d of the sketch is typically much smaller than the total dimension mn of the matrix $\boldsymbol{A}$. In this case, the sketching map $\mathcal{L}$ has a substantial null space. Therefore, it is natural to draw the sketching map *at random* so that we are likely to extract useful information from any fixed input matrix.

1.3. The Single View Paradigm. Notice that we can compute a sketch of the form (1.2) by scanning through the entries of the matrix $\boldsymbol{A}$ once in any order. One may visualize reading the matrix off of a tape without rewinding (for those who remember what a tape is). As a consequence, the sketching technique (1.2) is an example of a *single-view* or *single-pass* data access model.

There are (at least) two situations where the single-view model arises. First, we can imagine a setting where $\boldsymbol{A}$ is a very large matrix stored out of core memory [14, Sec. 5.5]. The cost of data transfer may be significant enough that we can only afford to read the matrix into core memory once.

Second, we may encounter a setting where the matrix $\boldsymbol{A}$ is presented as an ordered sum of updates:

$$\boldsymbol{A} = \boldsymbol{H}_1 + \boldsymbol{H}_2 + \boldsymbol{H}_3 + \boldsymbol{H}_4 + \cdots .$$

We must discard each innovation $\boldsymbol{H}_i$ after it is processed. This is called a *streaming model* [19, 7, 25]. In this context, the linearity of the sketching map $\mathcal{L}$ is essential to maintain a representation of $\boldsymbol{A}$ through an arbitrary sequence of updates.

1.4. Desiderata. Our aim is to construct a random sketching map $\mathcal{L}$ that acquires enough information to solve the low-rank matrix approximation problem (1.1). We must also design algorithms that compute a reconstruction $\hat{\boldsymbol{A}}$ from the sketch S without direct access to the matrix $\boldsymbol{A}$ itself.

This paper is targeted toward the numerical linear algebra community, and our goals align with traditional concerns of this research field:

1. **Minimal sketch size.** We want to design a sketching map $\mathcal{L}$ that minimizes the size d of the sketch S to achieve approximations that satisfy (1.1). We must also be able to represent the sketching map with d units of storage.
2. **Practical algorithms.** We seek matrix reconstruction algorithms that are reliable, numerically stable, and efficient in terms of storage and computation.
3. **Preservation of structure.** The approximations should maintain structural properties of the input matrix, such as symmetry or positive-semidefiniteness.
4. **Error bounds.** We demand explicit *a priori* error bounds for the algorithms so we can determine a sketch size d that suffices to achieve a specific approximation goal.

Our focus on minimizing the sketch size d was motivated by a specific application in optimization [6]. In other applications, it may be more important to control the arithmetic cost of applying the sketching map $\mathcal{L}$ to a matrix $\boldsymbol{A}$. Unfortunately, there is some tension between these goals; see subsection 3.9. Other works, such as [26, 7], focus on the latter.

Remark 1.1 (The Frobenius Norm). The sketching model (1.2) makes it impossible to achieve relative error bounds with respect to the spectral norm [25, Sec. 6.1]. Therefore, we have chosen to work with the Frobenius norm, in contrast to most research in numerical linear algebra.

1.5. Our Approach and Contributions. This paper describes a family of single-view algorithms for low-rank matrix approximation that achieve the desiderata above. These methods are provably correct variants of the heuristic approaches described by Halko et al. [14, Sec. 5.5]. See subsection 1.6 for a more complete discussion of related work.

As an example of our results, we summarize the simplest low-rank reconstruction algorithm and its properties. Fix an input matrix $\boldsymbol{A} \in \mathbb{F}^{m\times n}$ and a target rank r. Select sketch size parameters k and ℓ. We acquire a (randomized) sketch of the form

$$\boldsymbol{Y} := \boldsymbol{A}\boldsymbol{\Omega} \quad \text{and} \quad \boldsymbol{W} := \boldsymbol{\Psi}\boldsymbol{A} \tag{1.3}$$

where $\boldsymbol{\Omega} \in \mathbb{F}^{n\times k}$ and $\boldsymbol{\Psi} \in \mathbb{F}^{\ell\times m}$ are independent standard normal matrices; see Definition 2.1. We can store the random matrices and the sketch using $(k+\ell)(m+n)$ scalars. The arithmetic cost of forming the sketch is $\Theta((k+\ell)mn)$ floating-point operations (flops) for a general matrix $\boldsymbol{A}$.

Given the random matrices $(\boldsymbol{\Omega}, \boldsymbol{\Psi})$ and the sketch $(\boldsymbol{Y}, \boldsymbol{W})$, we compute an approximation $\hat{\boldsymbol{A}}$ in three steps:

1. Form an orthogonal–triangular factorization $\boldsymbol{Y} =: \boldsymbol{Q}\boldsymbol{R}$ where $\boldsymbol{Q} \in \mathbb{F}^{m\times k}$.
2. Solve a least-squares problem to obtain $\boldsymbol{X} := (\boldsymbol{\Psi}\boldsymbol{Q})^{\dagger}\boldsymbol{W} \in \mathbb{F}^{k\times n}$.
3. Construct the rank-k approximation $\hat{\boldsymbol{A}} := \boldsymbol{Q}\boldsymbol{X}$.

The total cost of this computation is $\Theta(k\ell(m+n))$ flops.

Now, suppose that we set the sketch size parameters $k = 2r+1$ and $\ell = 4r+2$. For this choice, Theorem 4.1 yields the error bound

$$\mathbb{E}\,\|\boldsymbol{A} - \hat{\boldsymbol{A}}\|_{\mathrm{F}} \le 2 \cdot \min_{\operatorname{rank}\boldsymbol{Z}\le r} \|\boldsymbol{A} - \boldsymbol{Z}\|_{\mathrm{F}}.$$

In other words, we typically obtain an approximation with rank $\approx 2r$ whose error lies within twice the optimal rank-r error! Moreover, the total storage cost is about $6r(m+n)$, which is comparable with the number of degrees of freedom in an $m \times n$ matrix with rank r, so the sketch size cannot be reduced substantially.

The procedure above is the basis for a suite of other algorithms. We can produce approximations that have a specific structure (such as symmetry or positive semidefiniteness) by projecting the initial approximation $\hat{\boldsymbol{A}}$ onto the family of structured matrices. A similar idea allows us to deliver approximations whose rank does not exceed the target rank r. Each of these algorithms is accompanied by an explicit error bound that controls how the approximation quality depends on the sketch size parameters k and ℓ. We also include pseudocode and an analysis of computational costs.

1.6. Overview of Related Work. Randomized algorithms for matrix approximation date back to research [22, 12] in theoretical computer science (TCS) in the late 1990s. Starting around 2004, this work inspired numerical analysts to develop practical versions [17] of these algorithms. See the paper [14, Sec. 2] for a comprehensive historical discussion. The surveys [16, 25] provide more details about the development of these ideas within the TCS literature.

Many of the early randomized matrix approximation algorithms, such as [11, 17], only require a small number of views of the matrix. (That is, the algorithms scan sequentially through the entries of the matrix a small number of times.) Researchers only began to focus on minimizing the number of views in the late 2000s. In particular, the papers [26, 7] both describe how to develop single-view algorithms that have

provable guarantees. The paper [14, Sec. 5.5] also outlines a heuristic procedure for single-view matrix approximation; this treatment is the basis of our approach.

Most of the research on single-view algorithms has taken place within the TCS community. Beginning with a paper [23] of Sarlós, researchers identified an abstract primitive, called a *randomized subspace embedding*, that can be used to solve a variety of numerical linear algebra problems. The surveys [16, 25] elaborate on this idea. In particular, Woodruff [25, Thm. 4.3] has demonstrated that randomized subspace embeddings can be used to build single-view matrix approximation algorithms. See subsections 4.7 and 5.4 for more information on Woodruff's results.

There is a substantial body of research on designing randomized subspace embeddings. See subsection 3.9 for an overview.

The sketch (1.3) is an example of a randomized subspace embedding. In contrast to earlier work, our analysis is *not* based on the randomized subspace embedding abstraction. We have developed a new approach that provides sharp error bounds.

There are several key features of this paper. First, we can guarantee that our sketches are essentially as small as possible (including the numerical constants). Second, we demonstrate that our algorithms that are reliable, practical, and numerically stable. Third, we have introduced a new framework for computing structured approximations. Last, we have provided the first concrete error bounds that can be used to select algorithm parameters.

2. Background.

In this section, we collect notation and conventions, as well as some background on random matrices.

2.1. Notation and Conventions.

We write $\mathbb{F}$ for the scalar field, which is either $\mathbb{R}$ or $\mathbb{C}$. The letter $\mathbf{I}$ signifies the identity matrix; its dimensions are determined by context. The star * refers to the (conjugate) transpose operation on vectors and matrices. The dagger † is the Moore–Penrose pseudoinverse.

The symbol $\|\cdot\|_{\mathrm{F}}$ denotes the Frobenius norm, while $\langle\cdot,\cdot\rangle$ is the Frobenius inner product. We write $\|\cdot\|$ for the spectral norm.

The expression "$\boldsymbol{M}$ has rank r" and its variants mean that the rank of $\boldsymbol{M}$ does not exceed r. The symbol $[\![\boldsymbol{M}]\!]_r$ represents an optimal rank-r approximation of $\boldsymbol{M}$ with respect to Frobenius norm; this approximation need not be unique [15, Sec. 6].

The symbol $\mathbb{E}$ denotes expectation with respect to all random variables. For a given random variable Z, we write $\mathbb{E}_Z$ to denote expectation with respect to the randomness in Z only. Nonlinear functions bind before the expectation.

In the description of algorithms in the text, we primarily use standard mathematical notation. In the pseudocode, we also make use of some MATLAB R2016A functions in an effort to make the presentation more succinct.

We use the computer science interpretation of the $\mathcal{O}(\cdot)$ and $\Omega(\cdot)$ symbols to describe classes of functions that are bounded above or below up to constants. The class $\Theta(\cdot)$ consists of functions with the specified asymptotic growth.

2.2. Standard Normal Matrices.

Let us define an ensemble of random matrices that plays a central role in this work.

DEFINITION 2.1 (Standard Normal Matrix). *A matrix $\boldsymbol{G} \in \mathbb{R}^{m\times n}$ has the real standard normal distribution if the entries form an independent family of standard normal random variables (i.e., Gaussian with mean zero and variance one).*

A matrix $\boldsymbol{G} \in \mathbb{C}^{m\times n}$ has the complex standard normal distribution if it has the form $\boldsymbol{G} = \boldsymbol{G}_1 + \mathrm{i}\boldsymbol{G}_2$ where $\boldsymbol{G}_1$ and $\boldsymbol{G}_2$ are independent, real standard normal matrices.

Standard normal matrices are also known as Gaussian matrices.

We introduce numbers α and β that reflect the field over which the random matrix is defined:

$$\alpha := \alpha(\mathbb{F}) := \begin{cases} 1, & \mathbb{F} = \mathbb{R} \\ 0, & \mathbb{F} = \mathbb{C} \end{cases} \quad \text{and} \quad \beta := \beta(\mathbb{F}) := \begin{cases} 1, & \mathbb{F} = \mathbb{R} \\ 2, & \mathbb{F} = \mathbb{C} \end{cases}. \tag{2.1}$$

This notation allows us to treat the real and complex case simultaneously. The number β is a standard parameter in random matrix theory.

3. Sketching the Target Matrix. First, we discuss how to collect sufficient data about a target matrix to compute a low-rank reconstruction. Following [14, Sec. 5.5], we summarize the matrix by multiplying it on the right and the left by random test matrices. The dimension and distribution of these random test matrices together determine the potential accuracy of our reconstruction.

3.1. The Target Matrix. Let $\boldsymbol{A} \in \mathbb{F}^{m \times n}$ be a matrix that we wish to approximate. Our algorithms work regardless of the relative dimensions of $\boldsymbol{A}$, but there may sometimes be small benefits if we apply them to $\boldsymbol{A}^*$ instead.

3.2. The Target Rank. Let r be a target rank parameter with $1 \leq r \leq \min\{m, n\}$. We aim to construct a low-rank approximation of $\boldsymbol{A}$ whose error is close to the optimal rank-r error. We explicitly allow reconstructions with rank somewhat larger than r because they may be significantly more accurate.

In the single-view setting, the practitioner must use prior knowledge about the target matrix $\boldsymbol{A}$ to determine a target rank r that will result in satisfactory error guarantees. This decision is outside the scope of our work.

3.3. Parameters for the Sketch. Our sketch consists of two parts: a summary of the range of $\boldsymbol{A}$ and a summary of the co-range. The parameter k controls the size of the range sketch, and the parameter ℓ controls the size of the co-range sketch. They should satisfy the conditions

$$r \leq k \leq \ell \quad \text{and} \quad k \leq n \quad \text{and} \quad \ell \leq m. \tag{3.1}$$

In practice, we typically choose $k \approx r$ and $\ell \approx k$. See (4.6) and subsection 10.5 below.

The parameters k and ℓ do not play symmetrical roles. The smaller parameter k controls the rank of our approximations. Larger values of both k and ℓ result in better approximations at the cost of more storage and arithmetic. We quantify these tradeoffs in the sequel.

3.4. The Test Matrices. To form the sketch of the target matrix, we draw and fix two (random) test matrices:

$$\boldsymbol{\Omega} \in \mathbb{F}^{n \times k} \quad \text{and} \quad \boldsymbol{\Psi} \in \mathbb{F}^{\ell \times m}. \tag{3.2}$$

This paper contains a detailed analysis of the case where the test matrices are statistically independent and follow the standard normal distribution. Subsection 3.9 describes other potential distributions for the test matrices. Throughout the presentation, we state explicitly when we are making distributional assumptions on the test matrices.

3.5. The Sketch. The sketch of the target matrix $\boldsymbol{A} \in \mathbb{F}^{m \times n}$ consists of two matrices:

$$\boldsymbol{Y} := \boldsymbol{A}\boldsymbol{\Omega} \in \mathbb{F}^{m \times k} \quad \text{and} \quad \boldsymbol{W} := \boldsymbol{\Psi}\boldsymbol{A} \in \mathbb{F}^{\ell \times n}. \tag{3.3}$$

Algorithm 1 *Randomized Single-View Sketch.* Implements (3.2) and (3.3).

Require: Input matrix $\boldsymbol{A} \in \mathbb{F}^{m\times n}$; sketch size parameters $k \leq \ell$
Ensure: Constructs test matrices $\boldsymbol{\Omega} \in \mathbb{F}^{n\times k}$ and $\boldsymbol{\Psi} \in \mathbb{F}^{\ell\times m}$, range sketch $\boldsymbol{Y} = \boldsymbol{A\Omega} \in \mathbb{F}^{m\times k}$, and co-range sketch $\boldsymbol{W} = \boldsymbol{\Psi A} \in \mathbb{F}^{\ell\times n}$ as private variables

private: $\boldsymbol{\Omega}, \boldsymbol{\Psi}, \boldsymbol{Y}, \boldsymbol{W}$ ▷ Internal variables for SKETCH object ▷ Accessible to all SKETCH methods

function SKETCH($\boldsymbol{A}; k, \ell$) ▷ Constructor
  if $\mathbb{F} = \mathbb{R}$ **then**
    $\boldsymbol{\Omega} \leftarrow \texttt{randn}(n, k)$
    $\boldsymbol{\Psi} \leftarrow \texttt{randn}(\ell, m)$
  if $\mathbb{F} = \mathbb{C}$ **then**
    $\boldsymbol{\Omega} \leftarrow \texttt{randn}(n, k) + \texttt{i}\,\texttt{randn}(n, k)$
    $\boldsymbol{\Psi} \leftarrow \texttt{randn}(\ell, m) + \texttt{i}\,\texttt{randn}(\ell, m)$
  $\boldsymbol{\Omega} \leftarrow \texttt{orth}(\boldsymbol{\Omega})$ ▷ (optional) Improve numerical stability
  $\boldsymbol{\Psi}^* \leftarrow \texttt{orth}(\boldsymbol{\Psi}^*)$ ▷ (optional) Improve numerical stability
  $\boldsymbol{Y} \leftarrow \boldsymbol{A\Omega}$
  $\boldsymbol{W} \leftarrow \boldsymbol{\Psi A}$

The matrix $\boldsymbol{Y}$ collects information about the action of $\boldsymbol{A}$, while the matrix $\boldsymbol{W}$ collects information about the action of $\boldsymbol{A}^*$. Both parts are necessary.

This type of sketch is not new. The single-view approximation techniques in [14, Sec. 5.5] and [25, Thm. 4.3] both rely on a sketch of the form (3.3).

3.6. The Sketch as an Abstract Data Type. We present the sketch as an abstract data type using ideas from object-oriented programming. SKETCH is an object that contains information about a specific matrix $\boldsymbol{A}$. The test matrices $(\boldsymbol{\Omega}, \boldsymbol{\Psi})$ and the sketch matrices $(\boldsymbol{Y}, \boldsymbol{W})$ are private variables that are only accessible to the SKETCH methods. A user interacts with the SKETCH object by initializing it with a specific matrix and by applying linear updates. The user can also query the SKETCH object to obtain an approximation of the matrix $\boldsymbol{A}$ with specific properties. The individual algorithms described in this paper are all methods that belong to the SKETCH object.

3.7. Initializing the Sketch and its Costs. See Algorithm 1 for pseudocode that implements the sketching procedure (3.2) and (3.3) with either standard normal test matrices (default) or random orthonormal test matrices (optional steps). Note that the orthogonalization step requires additional arithmetic and communication.

The storage cost for the sketch $(\boldsymbol{Y}, \boldsymbol{W})$ is $mk + \ell n$ floating-point numbers in the field $\mathbb{F}$. The storage cost for two standard normal test matrices is $nk + \ell m$ floating point numbers in $\mathbb{F}$. Some other types of test matrices $(\boldsymbol{\Omega}, \boldsymbol{\Psi})$ have lower storage costs, but the sketch $(\boldsymbol{Y}, \boldsymbol{W})$ remains the same size.

For standard normal test matrices, the arithmetic cost of forming the sketch (3.3) is $\Theta((k + \ell)mn)$ flops when $\boldsymbol{A}$ is dense. If $\boldsymbol{A}$ is sparse, the cost is proportional to the number $\texttt{nnz}(\boldsymbol{A})$ of nonzero entries: $\Theta((k + \ell)\,\texttt{nnz}(\boldsymbol{A}))$ flops. Other types of test matrices sometimes yield lower arithmetic costs.

Algorithm 2 *Single-View Sketch: Linear Update.* Implements (3.6).

Require: Update matrix $\boldsymbol{H} \in \mathbb{F}^{m\times n}$; scalars $\theta, \eta \in \mathbb{F}$
Ensure: Modifies sketch $(\boldsymbol{Y}, \boldsymbol{W})$ to reflect linear update $\boldsymbol{A} \leftarrow \theta\boldsymbol{A} + \eta\boldsymbol{H}$

```
function SketchLinearUpdate(H; θ, η)
    Y ← θY + ηHΩ          ▷ Linear update to range sketch
    W ← θW + ηΨH          ▷ Linear update to co-range sketch
```

3.8. Processing Linear Updates. Suppose that the target matrix $\boldsymbol{A}$ is presented to us as a sequence of additive updates:

$$\boldsymbol{A} = \boldsymbol{H}_1 + \boldsymbol{H}_2 + \boldsymbol{H}_3 + \boldsymbol{H}_4 + \cdots. \tag{3.4}$$

This model includes the case where someone feeds us the matrix one entry at a time, or one row at a time, or one column at a time.

By exploiting linearity, we can incrementally construct the sketch (3.3) of the matrix $\boldsymbol{A}$ described by (3.4). We initialize the sketch with the zero matrix:

$$\boldsymbol{Y} \leftarrow \boldsymbol{0} \quad \text{and} \quad \boldsymbol{W} \leftarrow \boldsymbol{0}.$$

As each update $\boldsymbol{H} \in \mathbb{F}^{m\times n}$ arrives, we compute

$$\boldsymbol{Y} \leftarrow \boldsymbol{Y} + \boldsymbol{H}\boldsymbol{\Omega} \quad \text{and} \quad \boldsymbol{W} \leftarrow \boldsymbol{W} + \boldsymbol{\Psi}\boldsymbol{H}. \tag{3.5}$$

The arithmetic cost of each update depends on the cost of the matrix–matrix multiplications in (3.5). In particular, suppose that the test matrices $(\boldsymbol{\Omega}, \boldsymbol{\Psi})$ are stored explicitly and and the update is presented as a rank-one matrix $\boldsymbol{H} = \boldsymbol{u}\boldsymbol{v}^*$ where $\boldsymbol{u} \in \mathbb{F}^m$ and $\boldsymbol{v} \in \mathbb{F}^n$. Then we can update the sketch in $\mathcal{O}((k+\ell)(n+m))$ flops. Non-Gaussian test matrices may support faster updates in other special cases, e.g., when $\boldsymbol{H}$ is very sparse.

Our sketching model (3.3) also supports a more general linear update that is important for some applications [6]. Suppose the target matrix $\boldsymbol{A}$ is modified as

$$\boldsymbol{A} \leftarrow \theta\boldsymbol{A} + \eta\boldsymbol{H} \quad \text{where } \theta, \eta \in \mathbb{F}.$$

Then we update the sketch (3.3) via the rule

$$\boldsymbol{Y} \leftarrow \theta\boldsymbol{Y} + \eta\boldsymbol{H}\boldsymbol{\Omega} \quad \text{and} \quad \boldsymbol{W} \leftarrow \theta\boldsymbol{W} + \eta\boldsymbol{\Psi}\boldsymbol{H}. \tag{3.6}$$

Note that the arithmetic cost of this update is $\Omega(km + \ell n)$ because we have to rescale each entry of the sketch. See Algorithm 2 for pseudocode.

3.9. Choosing the Distribution of the Test Matrices. Our analysis is specialized to the case where the test matrices $\boldsymbol{\Omega}$ and $\boldsymbol{\Psi}$ are standard normal. But the sketch can be implemented using test matrices drawn from other distributions. The choice of distribution leads to some tradeoffs in the range of permissible parameters; the costs of randomness, arithmetic, and communication to generate the test matrices; the storage costs for the test matrices and the sketch; the arithmetic costs for sketching and updates; the numerical stability of reconstruction algorithms; and the quality of *a priori* error bounds.

Let us list some of the contending distributions along with background references. We have ranked these in decreasing order of reliability.

- **Orthonormal.** The optional steps in Algorithm 1 generate matrices $\boldsymbol{\Omega}$ and $\boldsymbol{\Psi}^*$ with orthonormal columns that span uniformly random subspaces of dimension k and ℓ. These matrices behave much like Gaussians, but they exhibit better numerical stability—especially when k and ℓ are large. For example, see [10].

- **Gaussian.** Following [17, 14], this paper focuses on test matrices with the standard normal distribution. Benefits include excellent practical performance and accurate *a priori* error bounds. Moreover, we can take the sketch sizes $k = \Theta(r)$ and $\ell = \Theta(r)$, which is the optimal scaling.

- **Rademacher.** These test matrices have independent Rademacher[1] entries. Their behavior is similar with standard normal test matrices, but there are minor improvements in the cost of storage and arithmetic, as well as the amount of randomness required. For example, see [7].

- **Subsampled Randomized Fourier Transform.** These test matrices take the form

$$\boldsymbol{\Omega} = \boldsymbol{D}_1 \boldsymbol{F}_1 \boldsymbol{P}_1 \quad \text{and} \quad \boldsymbol{\Psi} = \boldsymbol{P}_2 \boldsymbol{F}_2 \boldsymbol{D}_2$$

  where $\boldsymbol{D}_1 \in \mathbb{F}^{n\times n}$ and $\boldsymbol{D}_2 \in \mathbb{F}^{m\times m}$ are diagonal matrices with independent Rademacher entries; $\boldsymbol{F}_1 \in \mathbb{F}^{n\times n}$ and $\boldsymbol{F}_2 \in \mathbb{F}^{m\times m}$ are discrete cosine transform ($\mathbb{F} = \mathbb{R}$) or discrete Fourier transform ($\mathbb{F} = \mathbb{C}$) matrices; and $\boldsymbol{P}_1 \in \mathbb{F}^{n\times k}$ and $\boldsymbol{P}_2 \in \mathbb{F}^{\ell\times m}$ are restrictions onto k and ℓ coordinates, chosen uniformly at random. These matrices work well in practice; they require a modest amount of storage; and they support fast arithmetic. On the other hand, it is necessary and sufficient that the sketch size parameters satisfy $k = \Theta((r + \log n)\log r)$ and $\ell = \Theta((k + \log m)\log k)$ to guarantee proper performance. See [1, 26, 2, 14, 24, 4].

- **Ultra-Sparse Rademacher.** Let s be a sparsity parameter. In each row of $\boldsymbol{\Omega}$ and column of $\boldsymbol{\Psi}$, we place independent Rademacher random variables in s uniformly random locations; the remaining entries of the test matrices are zero. These matrices help control storage, arithmetic, and randomness costs. On the other hand, they are somewhat less reliable and numerically stable. At the minimum sparsity $s = 1$, it is necessary and sufficient that the sketch size parameters satisfy $k = \Theta(r^2)$ and $\ell = \Theta(r^4)$. When $s = \Theta(\log r)$, it is sufficient that $k = \mathcal{O}(r \log r)$ and $\ell = \mathcal{O}(r \log^2 r)$. For more details, see [8, 20, 18, 21, 25, 3, 9].

An exhaustive comparison of distributions for the test matrices is outside the scope of this paper.

4. Low-Rank Approximation from a Single View. Suppose that we have acquired a sketch $(\boldsymbol{Y}, \boldsymbol{W})$ of the target matrix $\boldsymbol{A}$, as in (3.2) and (3.3). This section presents the most basic algorithm for computing a low-rank approximation of $\boldsymbol{A}$ from the data in the sketch.

In section 5, we describe modifications of this algorithm that produce approximations with fixed rank. In sections 6 and 7, we explain how to refine these procedures to obtain approximations with additional structure. Throughout, we maintain the notation of section 3.

[1] A Rademacher random variable takes the values ± 1 with equal probability.

4.1. The Basic Reconstruction Algorithm. Our goal is to produce a low-rank approximation of the target matrix $\boldsymbol{A}$ using only the knowledge of the test matrices $(\boldsymbol{\Omega}, \boldsymbol{\Psi})$ and the sketch $(\boldsymbol{Y}, \boldsymbol{W})$.

The first step in the reconstruction is to compute an orthobasis $\boldsymbol{Q}$ for the range of $\boldsymbol{Y}$ by means of an orthogonal–triangular factorization:

$$\boldsymbol{Y} =: \boldsymbol{Q}\boldsymbol{R} \quad \text{where} \quad \boldsymbol{Q} \in \mathbb{F}^{m \times k}. \tag{4.1}$$

The matrix $\boldsymbol{Q}$ has orthonormal columns; we discard the triangular matrix $\boldsymbol{R}$. The second step uses the co-range sketch $\boldsymbol{W}$ to form the matrix

$$\boldsymbol{X} := (\boldsymbol{\Psi}\boldsymbol{Q})^{\dagger}\boldsymbol{W} \in \mathbb{F}^{k \times n}. \tag{4.2}$$

We can perform this computation accurately because the random matrix $\boldsymbol{\Psi}\boldsymbol{Q} \in \mathbb{F}^{\ell \times k}$ is very well-conditioned when $\ell \gg k$. We report the rank-k approximation

$$\hat{\boldsymbol{A}} := \boldsymbol{Q}\boldsymbol{X} \in \mathbb{F}^{m \times n} \quad \text{where} \quad \boldsymbol{Q} \in \mathbb{F}^{m \times k} \quad \text{and} \quad \boldsymbol{X} \in \mathbb{F}^{k \times n}. \tag{4.3}$$

The factors $\boldsymbol{Q}$ and $\boldsymbol{X}$ are defined in (4.1) and (4.2).

4.2. Intuition. To motivate the algorithm, we recall a familiar heuristic [14, Sec. 1] from randomized linear algebra, which states that

$$\boldsymbol{A} \approx \boldsymbol{Q}\boldsymbol{Q}^{*}\boldsymbol{A}. \tag{4.4}$$

Although we would like to form the rank-k approximation $\boldsymbol{Q}(\boldsymbol{Q}^{*}\boldsymbol{A})$, we cannot compute the factor $\boldsymbol{Q}^{*}\boldsymbol{A}$ without revisiting the target matrix $\boldsymbol{A}$. Instead, we exploit the information in the co-range sketch $\boldsymbol{W} = \boldsymbol{\Psi}\boldsymbol{A}$. Notice that

$$\boldsymbol{W} = \boldsymbol{\Psi}(\boldsymbol{Q}\boldsymbol{Q}^{*}\boldsymbol{A}) + \boldsymbol{\Psi}(\boldsymbol{A} - \boldsymbol{Q}\boldsymbol{Q}^{*}\boldsymbol{A}) \approx (\boldsymbol{\Psi}\boldsymbol{Q})(\boldsymbol{Q}^{*}\boldsymbol{A}).$$

The heuristic (4.4) justifies dropping the second term. Multiplying on the left by the pseudoinverse $(\boldsymbol{\Psi}\boldsymbol{Q})^{\dagger}$, we arrive at the relation

$$\boldsymbol{X} = (\boldsymbol{\Psi}\boldsymbol{Q})^{\dagger}\boldsymbol{W} \approx \boldsymbol{Q}^{*}\boldsymbol{A}.$$

These considerations suggest that

$$\hat{\boldsymbol{A}} = \boldsymbol{Q}\boldsymbol{X} \approx \boldsymbol{Q}\boldsymbol{Q}^{*}\boldsymbol{A} \approx \boldsymbol{A}.$$

This explanation is inspired by the discussion in [14, Sec. 5.5]. One of our main contributions is to give substance to these nebulae.

4.3. Algorithm and Costs. Algorithms 3 and 4 give pseudocode for computing the approximation (4.3). The first presentation uses MATLAB functions to abbreviate some of the steps, while the second includes more implementation details. Note that the use of the `orth` command may result in an approximation with rank q for some $q \leq k$, but the quality of the approximation does not change.

Let us summarize the costs of the reconstruction procedure (4.1)–(4.3), as implemented in Algorithm 4. The algorithm has working storage of $\mathcal{O}(k(m+n))$ floating point numbers. The arithmetic cost is $\Theta(k\ell(m+n))$ flops, which is dominated by the matrix–matrix multiplications. The orthogonalization step and the back-substitution cost $\Theta(k^2(m+n))$ flops, which is almost as significant.

Algorithm 3 *Simplest Single-View Low-Rank Approximation.* Implements (4.3).

Ensure: For some $q \leq k$, returns factors $\boldsymbol{Q} \in \mathbb{F}^{m \times q}$ with orthonormal columns and $\boldsymbol{X} \in \mathbb{F}^{q \times n}$ that form a rank-q approximation $\hat{\boldsymbol{A}}_{\text{out}} = \boldsymbol{Q}\boldsymbol{X}$ of the sketched matrix

```
function SketchSimpleLowRankApprox( )
    Q ← orth(Y)                          ▷ Orthobasis for range of Y
    X ← (ΨQ)\W                           ▷ Multiply (ΨQ)^† on left side of W
    return (Q, X)
```

Algorithm 4 *Single-View Low-Rank Approximation.* Implements (4.3).

Ensure: Returns factors $\boldsymbol{Q} \in \mathbb{F}^{m \times k}$ with orthonormal columns and $\boldsymbol{X} \in \mathbb{F}^{k \times n}$ that form a rank-k approximation $\hat{\boldsymbol{A}}_{\text{out}} = \boldsymbol{Q}\boldsymbol{X}$ of the sketched matrix

```
function SketchLowRankApprox( )
    (Q, ∼) ← qr(Y, 0)                    ▷ Orthobasis for range of Y
    (U, T) ← qr(ΨQ)                      ▷ Orthogonal–triangular factorization
    X ← T^{-1}(U*W)                      ▷ Apply inverse by back-substitution
    return (Q, X)
```

4.4. A Bound for the Frobenius-Norm Error. We have established a very accurate error bound for the approximation (4.3) that is implemented in Algorithms 3 and 4. This estimate is one of the key contributions of this paper.

Before stating the result, let us introduce a function that we use to simplify many of our error bounds. Recall that α is given by (2.1), and define

$$f(s,t) := \frac{s}{t - s - \alpha} \quad \text{for integers that satisfy } t > s + \alpha > \alpha. \tag{4.5}$$

Observe that the function $f(s, \cdot)$ is decreasing, with range $(0, s]$.

THEOREM 4.1 (Low-Rank Approximation: Frobenius Error). *Assume the sketch size parameters satisfy $k > r + \alpha$ and $\ell > k + \alpha$. Draw random test matrices $\boldsymbol{\Omega} \in \mathbb{F}^{n \times k}$ and $\boldsymbol{\Psi} \in \mathbb{F}^{\ell \times m}$ independently from the standard normal distribution. Then the rank-k approximation $\hat{\boldsymbol{A}}$ obtained from formula (4.3) satisfies*

$$\mathbb{E}\, \|\boldsymbol{A} - \hat{\boldsymbol{A}}\|_{\text{F}}^2 \leq (1 + f(r,k))(1 + f(k,\ell)) \cdot \|\boldsymbol{A} - [\![\boldsymbol{A}]\!]_r\|_{\text{F}}^2.$$

The function f is defined in (4.5), and α is given by (2.1).

The proof of Theorem 4.1 appears below in subsection 8.3.

The error bound in Theorem 4.1 is precise enough to predict the actual performance of the approximation (4.3). As a consequence, we can use the result to make *a priori* decisions about the best sketch size parameters (k, ℓ). See section 10.

To appreciate the meaning of Theorem 4.1, it is helpful to consider specific choices for the sketch size parameters. First, notice that the selection

$$k = 2r + \alpha \quad \text{and} \quad \ell = 2k + \alpha \tag{4.6}$$

yields the error bound

$$\left(\mathbb{E}\, \|\boldsymbol{A} - \hat{\boldsymbol{A}}\|_{\text{F}}^2\right)^{1/2} \leq 2 \cdot \|\boldsymbol{A} - [\![\boldsymbol{A}]\!]_r\|_{\text{F}}.$$

In other words, for $k \approx 2r$, we can construct a rank-k approximation of $\boldsymbol{A}$ that has almost the same quality as the best rank-r approximation. We recommend the parameter choice (4.6) because it achieves a good tradeoff between the size of the sketch and the accuracy of the reconstruction.

Next, observe that for fixed $s > 0$ and $\varepsilon > 0$, we have

$$f(s, (1+\varepsilon^{-1})s + \alpha) = \varepsilon.$$

Therefore, for any choice of s, we can make the function $t \mapsto f(s,t)$ arbitrarily small by increasing t. Roughly speaking, we need $t \approx s/\varepsilon$ to achieve the bound $f(s,t) \approx \varepsilon$. In particular, suppose that we set

$$k = (1+\varepsilon^{-1})r + \alpha \quad \text{and} \quad \ell = (1+\varepsilon^{-1})k + \alpha.$$

Then we achieve the error bound

$$\left(\mathbb{E}\,\|\boldsymbol{A} - \hat{\boldsymbol{A}}\|_{\mathrm{F}}^2\right)^{1/2} \le (1+\varepsilon) \cdot \|\boldsymbol{A} - [\![\boldsymbol{A}]\!]_r\|_{\mathrm{F}}.$$

Thus, the choices $k \approx r/\varepsilon$ and $\ell \approx r/\varepsilon^2$ suffice to obtain a relative error of $1+\varepsilon$.

4.5. A Bound for the Spectral-Norm Error. For reference, we include a bound on the approximation error that the reconstruction (4.3) achieves with respect to the spectral norm. The form of this bound is essentially correct, but the constants are not sharp. For brevity, we have only developed this result for the real field.

It is helpful to introduce two more functions to simplify the estimate. Let

$$g(s,t) := 1 + \sqrt{\frac{s}{t-s-1}} \quad \text{and} \quad h(s,t) := \frac{\mathrm{e}\sqrt{t}}{t-s} \quad \text{for integers } t > s+1 > 1. \tag{4.7}$$

The function $g(s,\cdot)$ is decreasing with range $(1, 1+\sqrt{s}]$, and the function $h(s,\cdot)$ is decreasing with range $(0, (\mathrm{e}/2)\sqrt{s+2}]$.

THEOREM 4.2 (Low-Rank Reconstruction: Spectral Error). *Assume the sketch size parameters satisfy $k > r+1$ and $\ell > r+1$. Draw random test matrices $\boldsymbol{\Omega} \in \mathbb{R}^{n\times k}$ and $\boldsymbol{\Psi} \in \mathbb{R}^{\ell\times m}$ independently from the real standard normal distribution. Then the rank-k approximation $\hat{\boldsymbol{A}}$ obtained from the formula (4.3) satisfies*

$$\begin{aligned}\mathbb{E}\,\|\boldsymbol{A} - \hat{\boldsymbol{A}}\| &\le g(r,k) \cdot g(k,\ell) \cdot \|\boldsymbol{A} - [\![\boldsymbol{A}]\!]_r\| \\ &\quad + \big[h(r,k) \cdot g(k,\ell) + g(r,k) \cdot h(k,\ell)\big] \cdot \|\boldsymbol{A} - [\![\boldsymbol{A}]\!]_r\|_{\mathrm{F}}.\end{aligned} \tag{4.8}$$

The functions g and h are defined in (4.7).

The proof of Theorem 4.2 appears below in subsection 8.4.

To appreciate the meaning of this result, we consider specific choices for k and ℓ. In particular, our recommended parameter selection (4.6) delivers the error bound

$$\mathbb{E}\,\|\boldsymbol{A} - \hat{\boldsymbol{A}}\| \le 4 \cdot \|\boldsymbol{A} - [\![\boldsymbol{A}]\!]_r\| + \frac{4\mathrm{e}\sqrt{2}}{\sqrt{r}} \cdot \|\boldsymbol{A} - [\![\boldsymbol{A}]\!]_r\|_{\mathrm{F}}$$

Note that the Frobenius-norm error term is scaled by a factor of $r^{-1/2}$, so it plays a less significant role as the target rank r increases. One interpretation is that the part of the matrix we fail to approximate behaves like noise that is spread evenly across the singular vectors of the approximation.

It is unpalatable to find a Frobenius-norm term in our bound (4.8) on the spectral-norm error, but we have to swallow it. Indeed, there are lower bounds [25, Sec. 6.2] that prevent us from obtaining a constant-factor approximation to the spectral-norm error unless the size of the sketch is comparable with the matrix dimensions: $k = \Omega(\min\{m, n\})$.

4.6. High-Probability Error Bounds. The expectation bounds presented in Theorems 4.1 and 4.2 also describe the typical behavior of the algorithm (4.3) because of measure concentration effects. It is possible to develop high-probability bounds using the methods from [14, Sec. 10.3]. We have chosen to omit these results. They are similar in spirit with [14, Thm. 10.7 and 10.8], but they are more complicated without providing any additional insight.

4.7. Comparison with Prior Work. We developed the sketch (3.3) and the approximation procedure (4.3) independently, with inspiration from the discussion in [14, Sec. 5.5]. We later discovered that the reconstruction (4.3) is algebraically equivalent to a formula [25, Thm. 4.3, display 1] proposed by Woodruff. In our notation, his reconstruction takes the form

$$\hat{\boldsymbol{A}}_{\mathrm{woo1}} := \boldsymbol{Y}(\boldsymbol{\Psi}\boldsymbol{Y})^{\dagger}\boldsymbol{W} = \boldsymbol{Y}(\boldsymbol{W}\boldsymbol{\Omega})^{\dagger}\boldsymbol{W}. \tag{4.9}$$

In floating-point arithmetic, our approximation (4.3), implemented in Algorithms 3 and 4, is superior to (4.9). The analysis in Theorems 4.1 and 4.2 is new. We also give the first concrete guidance on selecting the parameters k and ℓ.

5. Fixed-Rank Approximation from a Single View. In some situations, we need to approximate the target matrix by a matrix with fixed rank. Although the simple reconstruction (4.3) from section 4 produces a rank-k matrix, we may need to reduce the rank to match the target rank r. In this section, we explain how to obtain a rank-r approximation by projecting the simple reconstruction onto the set of rank-r matrices. We argue that this procedure only increases the error by limited amount.

5.1. The Fixed-Rank Reconstruction Algorithm. Suppose that we wish to compute a rank-r approximation of the target matrix $\boldsymbol{A} \in \mathbb{F}^{m\times n}$. First, we form an initial approximation $\hat{\boldsymbol{A}} := \boldsymbol{Q}\boldsymbol{X}$ using the procedure (4.3). Then we obtain a rank-r approximation $[\![\hat{\boldsymbol{A}}]\!]_r$ of the target matrix by replacing $\hat{\boldsymbol{A}}$ with its best rank-r approximation in Frobenius norm:

$$[\![\hat{\boldsymbol{A}}]\!]_r = [\![\boldsymbol{Q}\boldsymbol{X}]\!]_r. \tag{5.1}$$

We can complete this operation by working directly with the factors. Indeed, suppose that $\boldsymbol{X} = \boldsymbol{U}\boldsymbol{\Sigma}\boldsymbol{V}^*$ is an SVD of $\boldsymbol{X}$. Then $\boldsymbol{Q}\boldsymbol{X}$ has an SVD of the form

$$\boldsymbol{Q}\boldsymbol{X} = (\boldsymbol{Q}\boldsymbol{U})\boldsymbol{\Sigma}\boldsymbol{V}^*.$$

As such, there is also a best rank-r approximation of $\boldsymbol{Q}\boldsymbol{X}$ that satisfies

$$[\![\boldsymbol{Q}\boldsymbol{X}]\!]_r = (\boldsymbol{Q}\boldsymbol{U})[\![\boldsymbol{\Sigma}]\!]_r\boldsymbol{V}^* = \boldsymbol{Q}[\![\boldsymbol{X}]\!]_r.$$

Therefore, the desired rank-r approximation (5.1) can also be expressed as

$$[\![\hat{\boldsymbol{A}}]\!]_r = \boldsymbol{Q}[\![\boldsymbol{X}]\!]_r. \tag{5.2}$$

The formula (5.2) is more computationally efficient than (5.1) because the factor $\boldsymbol{X} \in \mathbb{F}^{k\times n}$ is much smaller than the approximation $\hat{\boldsymbol{A}} \in \mathbb{F}^{m\times n}$.

Algorithm 5 *Single-View Fixed-Rank Approximation.* Implements (5.2).

Require: Target rank $r \leq k$

Ensure: Returns factors $\boldsymbol{Q} \in \mathbb{F}^{m\times r}$ and $\boldsymbol{V} \in \mathbb{F}^{n\times r}$ with orthonormal columns and nonnegative diagonal $\boldsymbol{\Sigma} \in \mathbb{F}^{r\times r}$ that form a rank-r approximation $\hat{\boldsymbol{A}}_{\text{out}} = \boldsymbol{Q}\boldsymbol{\Sigma}\boldsymbol{V}^*$ of the sketched matrix

```
function SKETCH.FIXEDRANKAPPROX(r)
    (Q, X) ← LOWRANKAPPROX( )                ▷ Get Â_in = QX
    (U, Σ, V) ← svds(X, r)                   ▷ Form full SVD and truncate
    Q ← QU                                   ▷ Consolidate orthonormal factors
    return (Q, Σ, V)
```

5.2. Algorithm and Costs. Algorithm 5 contains pseudocode for computing the fixed-rank approximation (5.2).

The fixed-rank reconstruction in Algorithm 5 has storage and arithmetic costs on the same order as the simple low-rank reconstruction (Algorithm 3). Indeed, to compute the truncated SVD and perform the matrix–matrix multiplication, we expend only $\Theta(k^2 n)$ additional flops. Thus, the total working storage is $\Theta(k(m+n))$ numbers and the arithmetic cost is $\Theta(k\ell(m+n))$ flops.

5.3. A Bound on the Frobenius-Norm Error. We have established an error bound for the rank-r approximation (5.2) implemented in Algorithm 5. This estimate is helpful because it has small and explicit constants, even though it less precise than the analysis in Theorem 4.1.

THEOREM 5.1 (Fixed-Rank Reconstruction: Frobenius-Norm Error). *Assume the sketch size parameters satisfy $k > r+\alpha$ and $\ell > k+\alpha$. Draw random test matrices $\boldsymbol{\Omega} \in \mathbb{F}^{n\times k}$ and $\boldsymbol{\Psi} \in \mathbb{F}^{\ell\times m}$ independently from the standard normal distribution. Then the rank-r approximation $[\![\hat{\boldsymbol{A}}]\!]_r$ obtained from the formula (5.2) satisfies*

$$\mathbb{E}\,\|\boldsymbol{A} - [\![\hat{\boldsymbol{A}}]\!]_r\|_{\mathrm{F}} \leq \sqrt{1+f(r,k)}\big(1+2\sqrt{f(k,\ell)}\big)\cdot\|\boldsymbol{A}-[\![\boldsymbol{A}]\!]_r\|_{\mathrm{F}}. \tag{5.3}$$

The function f is defined in (4.5), and the number α is given by (2.1).

The proof of Theorem 5.1 appears in section 9.

It is valuable to consider specific choices for the sketch size (k,ℓ). Our recommended selection (4.6) gives the bound

$$\mathbb{E}\,\|\boldsymbol{A} - [\![\hat{\boldsymbol{A}}]\!]_r\|_{\mathrm{F}} \leq 3\sqrt{2}\cdot\|\boldsymbol{A}-[\![\boldsymbol{A}]\!]_r\|_{\mathrm{F}}.$$

Moreover, for any tolerance $\varepsilon > 0$, we can set $k \approx r/\varepsilon$ and $\ell \approx r/\varepsilon^3$ to drive the leading constant in (5.3) down to $1+\varepsilon$.

We believe that the fixed-rank reconstruction (5.2) behaves better than the error bound (5.3) predicts. It is likely that $\ell \approx r/\varepsilon^2$ suffices to achieve a relative error of $1+\varepsilon$, but we were not able to obtain conclusive evidence in support of this point.

5.4. Comparison with Prior Work. The theoretical computer science (TCS) literature contains a substantial amount of research on single-view fixed-rank approximation. In particular, Woodruff [25, Thm. 4.3, display 2] has proposed a related reconstruction method. First, he forms a matrix product and computes its orthogonal–triangular factorization:

$$\boldsymbol{B} := \boldsymbol{\Psi}\boldsymbol{Y} \quad\text{and}\quad \boldsymbol{B} =: \boldsymbol{U}\boldsymbol{R} \quad\text{where}\quad \boldsymbol{U} \in \mathbb{F}^{\ell\times k}. \tag{5.4}$$

Then he constructs the approximation

$$\hat{\boldsymbol{A}}_{\mathrm{woo2}} := \boldsymbol{Y}(\boldsymbol{\Psi}\boldsymbol{Y})^{\dagger}\boldsymbol{U}[\![\boldsymbol{U}^*\boldsymbol{W}]\!]_r. \tag{5.5}$$

As it happens, there is only a limited difference between Woodruff's fixed-rank reconstruction formula (5.5) and our formula (5.2).

To explain, let us give an algebraically equivalent statement of the formula (5.5) that is better suited to floating-point arithmetic. First, we form a matrix product and compute its orthogonal–triangular factorization:

$$\boldsymbol{C} := \boldsymbol{\Psi}\boldsymbol{Q} \quad \text{and} \quad \boldsymbol{C} =: \boldsymbol{U}\boldsymbol{T} \quad \text{where} \quad \boldsymbol{U} \in \mathbb{F}^{\ell\times k}.$$

Algebraically, the matrix $\boldsymbol{U}$ here is equal to the one in (5.4). When $\ell \geq k$ and $\boldsymbol{\Psi}$ is standard normal, $\boldsymbol{T}$ is almost surely invertible. Woodruff's fixed-rank reconstruction (5.5) is algebraically (but not numerically) equivalent to

$$\hat{\boldsymbol{A}}_{\mathrm{woo2}'} := \boldsymbol{Q}\boldsymbol{T}^{-1}[\![\boldsymbol{U}^*\boldsymbol{W}]\!]_r. \tag{5.6}$$

For comparison, our reconstruction (5.2) can be written as

$$[\![\hat{\boldsymbol{A}}]\!]_r = \boldsymbol{Q}[\![\boldsymbol{T}^{-1}\boldsymbol{U}^*\boldsymbol{W}]\!]_r. \tag{5.7}$$

Numerical evidence suggests that our approach is superior, but neither one dominates for every example and choice of the parameters (r, k, ℓ). See section 10 for details.

We adapted Woodruff's analysis [25, Thm. 4.3] to study the behavior of the approximation (5.6) for standard normal test matrices. We were able to prove that the choices $k = \mathcal{O}(r/\varepsilon)$ and $\ell = \mathcal{O}(r/\varepsilon^3 + (\log n)/\varepsilon^2)$ are sufficient for (5.6) to achieve a relative error of $1+\varepsilon$. In contrast, Theorem 5.1, our analysis of the reconstruction (5.7), avoids the logarithmic term in the parameter ℓ.

6. Low-Rank Approximations with Convex Structure. In many instances, we wish to reconstruct a target matrix that has additional structure, such as symmetry or positive-semidefiniteness. The reconstruction formula (4.3) from section 4 produces an approximation that has no special properties aside from a bound on its rank. Therefore, we may need to refine our approximation to instill additional virtues.

In this section, we consider a class of problems where the target matrix belongs to a convex set and we seek an approximation that belongs to the same set. To accomplish this goal, we replace our initial approximation with the closest point in the convex set. This procedure always helps.

We address two specific examples: (i) the case where the target matrix is conjugate symmetric and (ii) the case where the target matrix is positive semidefinite. In both situations, we must design the reconstruction algorithm carefully to avoid forming full-size matrices.

6.1. Projection onto a Convex Set. Let C be a closed and convex set of matrices in $\mathbb{F}^{m\times n}$. Define the projector $\boldsymbol{\Pi}_C$ onto the set C to be the map

$$\boldsymbol{\Pi}_C : \mathbb{F}^{m\times n} \to C \quad \text{where} \quad \boldsymbol{\Pi}_C(\boldsymbol{M}) := \operatorname{argmin}\big\{\|\boldsymbol{C} - \boldsymbol{M}\|_{\mathrm{F}}^2 : \boldsymbol{C} \in C\big\}.$$

The argmin operator returns the matrix $\boldsymbol{C}_\star \in C$ that solves the optimization problem. The solution $\boldsymbol{C}_\star$ is uniquely determined because the squared Frobenius norm is strictly convex and the constraint set C is closed and convex.

6.2. Improved Approximation by Convex Projection. Suppose that the target matrix $\boldsymbol{A}$ belongs to the closed, convex set $C \subset \mathbb{F}^{m\times n}$. Let $\hat{\boldsymbol{A}}_{\text{in}} \in \mathbb{F}^{m\times n}$ be an initial approximation of $\boldsymbol{A}$. We can produce a new approximation $\boldsymbol{\Pi}_C(\hat{\boldsymbol{A}}_{\text{in}})$ by projecting the initial approximation onto the constraint set. This procedure always improves the approximation quality.

FACT 6.1 (Convex Structure Reduces Error). *Let $C \in \mathbb{F}^{m\times n}$ be a closed convex set, and suppose that $\boldsymbol{A} \in C$. For any initial approximation $\hat{\boldsymbol{A}}_{\text{in}} \in \mathbb{F}^{m\times n}$,*

$$\|\boldsymbol{A} - \boldsymbol{\Pi}_C(\hat{\boldsymbol{A}}_{\text{in}})\|_{\text{F}} \le \|\boldsymbol{A} - \hat{\boldsymbol{A}}_{\text{in}}\|_{\text{F}}. \tag{6.1}$$

This result is well known in convex analysis. It follows directly from the first-order optimality conditions [5, Sec. 4.2.3] for the Frobenius-norm projection of a matrix onto the set C. We omit the details.

6.3. Low-Rank Approximation with Conjugate Symmetry. When the target matrix is conjugate symmetric, it is often critical to produce a conjugate symmetric approximation. We can do so by combining the simple approximation from section 4 with the projection step outlined in subsection 6.1.

6.3.1. Conjugate Symmetric Projection. Define the set $\mathbb{H}^n(\mathbb{F})$ of conjugate symmetric matrices with dimension n over the field $\mathbb{F}$:

$$\mathbb{H}^n := \mathbb{H}^n(\mathbb{F}) := \{\boldsymbol{C} \in \mathbb{F}^{n\times n} : \boldsymbol{C} = \boldsymbol{C}^*\}.$$

The set $\mathbb{H}^n(\mathbb{F})$ is convex because it forms a real-linear subspace in $\mathbb{F}^{n\times n}$. In the sequel, we omit the field $\mathbb{F}$ from the notation unless there is a possibility of confusion.

The projection $\boldsymbol{M}_{\text{sym}}$ of a matrix $\boldsymbol{M} \in \mathbb{F}^{n\times n}$ onto the set $\mathbb{H}^n$ takes the form

$$\boldsymbol{M}_{\text{sym}} := \boldsymbol{\Pi}_{\mathbb{H}^n}(\boldsymbol{M}) = \frac{1}{2}(\boldsymbol{M} + \boldsymbol{M}^*). \tag{6.2}$$

For example, see [15, Sec. 2].

6.3.2. Computing a Conjugate Symmetric Approximation. Assume that the target matrix $\boldsymbol{A} \in \mathbb{H}^n$ is conjugate symmetric. Let $\hat{\boldsymbol{A}} := \boldsymbol{QX}$ be an initial rank-k approximation of $\boldsymbol{A}$ obtained from the reconstruction procedure (4.3). We can form a better approximation $\hat{\boldsymbol{A}}_{\text{sym}}$ by projecting $\hat{\boldsymbol{A}}$ onto $\mathbb{H}^n$:

$$\hat{\boldsymbol{A}}_{\text{sym}} := \boldsymbol{\Pi}_{\mathbb{H}^n}(\hat{\boldsymbol{A}}) = \frac{1}{2}(\hat{\boldsymbol{A}} + \hat{\boldsymbol{A}}^*) = \frac{1}{2}(\boldsymbol{QX} + \boldsymbol{X}^*\boldsymbol{Q}^*). \tag{6.3}$$

The second relation follows from (6.2).

In most cases, it is preferable to present the approximation (6.3) in factored form. To do so, we observe that

$$\frac{1}{2}(\boldsymbol{QX} + \boldsymbol{X}^*\boldsymbol{Q}^*) = \frac{1}{2}\begin{bmatrix}\boldsymbol{Q} & \boldsymbol{X}^*\end{bmatrix}\begin{bmatrix}\mathbf{0} & \mathbf{I}\\ \mathbf{I} & \mathbf{0}\end{bmatrix}\begin{bmatrix}\boldsymbol{Q} & \boldsymbol{X}^*\end{bmatrix}^*.$$

Concatenate $\boldsymbol{Q}$ and $\boldsymbol{X}^*$, and compute the orthogonal–triangular factorization

$$\begin{bmatrix}\boldsymbol{Q} & \boldsymbol{X}^*\end{bmatrix} =: \boldsymbol{U}\begin{bmatrix}\boldsymbol{T}_1 & \boldsymbol{T}_2\end{bmatrix} \quad \text{where} \quad \boldsymbol{U} \in \mathbb{F}^{n\times 2k} \text{ and } \boldsymbol{T}_1 \in \mathbb{F}^{2k\times k}. \tag{6.4}$$

Of course, we only need to orthogonalize the k columns of $\boldsymbol{X}^*$, which permits some computational efficiencies. Next, introduce the matrix

$$\boldsymbol{S} := \frac{1}{2}\begin{bmatrix}\boldsymbol{T}_1 & \boldsymbol{T}_2\end{bmatrix}\begin{bmatrix}\mathbf{0} & \mathbf{I}\\ \mathbf{I} & \mathbf{0}\end{bmatrix}\begin{bmatrix}\boldsymbol{T}_1 & \boldsymbol{T}_2\end{bmatrix}^* = \frac{1}{2}(\boldsymbol{T}_1\boldsymbol{T}_2^* + \boldsymbol{T}_2\boldsymbol{T}_1^*) \in \mathbb{F}^{2k\times 2k}. \tag{6.5}$$

Algorithm 6 *Single-View Low-Rank Symmetric Approximation.* Implements (6.6).

Require: Matrix dimensions $m = n$

Ensure: For $q = 2k$, returns factors $\boldsymbol{U} \in \mathbb{F}^{n \times q}$ with orthonormal columns and $\boldsymbol{S} \in \mathbb{H}^q$ that form a rank-q conjugate symmetric approximation $\hat{\boldsymbol{A}}_{\text{out}} = \boldsymbol{U}\boldsymbol{S}\boldsymbol{U}^*$ of the sketched matrix

function SKETCH.LOWRANKSYMAPPROX( )
  $(\boldsymbol{Q}, \boldsymbol{X}) \leftarrow$ LOWRANKAPPROX( ) ▷ Get $\hat{\boldsymbol{A}}_{\text{in}} = \boldsymbol{Q}\boldsymbol{X}$
  $(\boldsymbol{U}, \boldsymbol{T}) \leftarrow \mathtt{qr}([\boldsymbol{Q}, \boldsymbol{X}^*], \mathtt{0})$ ▷ Orthogonal factorization of concatenation
  $\boldsymbol{T}_1 \leftarrow \boldsymbol{T}(:, 1\!:\!k)$ and $\boldsymbol{T}_2 \leftarrow \boldsymbol{T}(:, (k+1)\!:\!(2k))$ ▷ Extract submatrices
  $\boldsymbol{S} \leftarrow (\boldsymbol{T}_1\boldsymbol{T}_2^* + \boldsymbol{T}_2\boldsymbol{T}_1^*)/2$ ▷ Symmetrize
  return $(\boldsymbol{U}, \boldsymbol{S})$ ▷ Return factors

Combine the last four displays to obtain the rank-$(2k)$ conjugate symmetric approximation

$$\hat{\boldsymbol{A}}_{\text{sym}} = \boldsymbol{U}\boldsymbol{S}\boldsymbol{U}^*. \tag{6.6}$$

From this expression, it is easy to obtain other types of factorizations, such as an eigenvalue decomposition, by further processing.

6.3.3. Algorithm and Costs. Algorithm 6 contains pseudocode for producing a conjugate symmetric reconstruction of the form (6.6) from a sketch of the target matrix. One can make this algorithm slightly more efficient by taking advantage of the fact that $\boldsymbol{Q}$ has orthogonal columns; we omit the details.

For Algorithm 6, the total working storage is $\Theta(kn)$ and the arithmetic cost is $\Theta(k\ell n)$. These costs are dominated by the call to SKETCH.LOWRANKAPPROX.

6.3.4. A Bound on the Frobenius-Norm Error. Combining Theorem 4.1 with Fact 6.1, we have the following bound on the error of the symmetric reconstruction (6.6), implemented in Algorithm 6.

COROLLARY 6.2 (Low-Rank Symmetric Reconstruction). *Assume that the target matrix $\boldsymbol{A} \in \mathbb{H}^n(\mathbb{F})$ is conjugate symmetric, and assume that the sketch size parameters satisfy $k > r + \alpha$ and $\ell > k + \alpha$. Draw random test matrices $\boldsymbol{\Omega} \in \mathbb{F}^{n \times k}$ and $\boldsymbol{\Psi} \in \mathbb{F}^{\ell \times n}$ independently from the standard normal distribution. Then the rank-$(2k)$ conjugate symmetric approximation $\hat{\boldsymbol{A}}_{\text{sym}}$ produced by (6.3) or (6.6) satisfies*

$$\mathbb{E}\,\|\boldsymbol{A} - \hat{\boldsymbol{A}}_{\text{sym}}\|_{\text{F}}^2 \le (1 + f(r,k))(1 + f(k,\ell)) \cdot \|\boldsymbol{A} - [\![\boldsymbol{A}]\!]_r\|_{\text{F}}^2.$$

The function f is defined in (4.5), and the number α is given by (2.1).

6.4. Low-Rank Positive-Semidefinite Approximation. We often encounter the problem of approximating a positive-semidefinite (psd) matrix. In many situations, it is important to produce an approximation that maintains positivity. Our approach combines the simple approximation (4.3) from section 4 with the projection step from subsection 6.1.

6.4.1. PSD Projection. We introduce the set $\mathbb{H}_+^n(\mathbb{F})$ of psd matrices with dimension n over the field $\mathbb{F}$:

$$\mathbb{H}_+^n := \mathbb{H}_+^n(\mathbb{F}) := \big\{\boldsymbol{C} \in \mathbb{H}^n : \boldsymbol{z}^*\boldsymbol{C}\boldsymbol{z} \ge 0 \text{ for each } \boldsymbol{z} \in \mathbb{F}^n\big\}.$$

Algorithm 7 *Single-View Low-Rank PSD Approximation.* Implements (6.7).

Require: Matrix dimensions $m = n$

Ensure: For $q = 2k$, returns factors $\boldsymbol{U} \in \mathbb{F}^{n \times q}$ with orthonormal columns and nonnegative, diagonal $\boldsymbol{D} \in \mathbb{H}_+^q$ that form a rank-q psd approximation $\hat{\boldsymbol{A}}_{\text{out}} = \boldsymbol{U}\boldsymbol{D}\boldsymbol{U}^*$ of the sketched matrix

```
function Sketch.LowRankPSDApprox( )
    (U, S) ← LowRankSymApprox( )          ▷ Get Â_in = USU*
    (V, D) ← eig(S)                       ▷ Form eigendecomposition
    U ← UV                                ▷ Consolidate orthonormal factors
    D ← max(D, 0)                         ▷ Zero out negative eigenvalues
    return (U, D)
```

The set $\mathbb{H}_+^n(\mathbb{F})$ is convex because it is an intersection of halfspaces. In the sequel, we omit the field $\mathbb{F}$ from the notation unless there is a possibility for confusion.

Given a matrix $\boldsymbol{M} \in \mathbb{F}^{n \times n}$, we construct its projection onto the set $\mathbb{H}_+^n$ in three steps. First, form the projection $\boldsymbol{M}_{\text{sym}} := \boldsymbol{\Pi}_{\mathbb{H}^n}(\boldsymbol{M})$ onto the conjugate symmetric matrices, as in (6.2). Second, compute an eigenvalue decomposition $\boldsymbol{M}_{\text{sym}} =: \boldsymbol{V}\boldsymbol{D}\boldsymbol{V}^*$. Third, form $\boldsymbol{D}_+$ by zeroing out the negative entries of $\boldsymbol{D}$. Then the projection $\boldsymbol{M}_+$ of the matrix $\boldsymbol{M}$ onto $\mathbb{H}_+^n$ takes the form

$$\boldsymbol{M}_+ := \boldsymbol{\Pi}_{\mathbb{H}_+^n}(\boldsymbol{M}) = \boldsymbol{V}\boldsymbol{D}_+\boldsymbol{V}^*.$$

For example, see [15, Sec. 3].

6.4.2. Computing a PSD Approximation. Assume that the target matrix $\boldsymbol{A} \in \mathbb{H}_+^n$ is psd. Let $\hat{\boldsymbol{A}} := \boldsymbol{Q}\boldsymbol{X}$ be an initial approximation of $\boldsymbol{A}$ obtained from the reconstruction procedure (4.3). We can form a psd approximation $\hat{\boldsymbol{A}}_+$ by projecting $\hat{\boldsymbol{A}}$ onto the set $\mathbb{H}_+^n$.

To do so, we repeat the computations (6.4) and (6.5) to obtain the symmetric approximation $\hat{\boldsymbol{A}}_{\text{sym}}$ presented in (6.6). Next, form an eigenvalue decomposition of the matrix $\boldsymbol{S}$ given by (6.5):

$$\boldsymbol{S} =: \boldsymbol{V}\boldsymbol{D}\boldsymbol{V}^*.$$

In view of (6.6), we obtain an eigenvalue decomposition of $\hat{\boldsymbol{A}}_{\text{sym}}$:

$$\hat{\boldsymbol{A}}_{\text{sym}} = (\boldsymbol{U}\boldsymbol{V})\boldsymbol{D}(\boldsymbol{U}\boldsymbol{V})^*.$$

To obtain the psd approximation $\hat{\boldsymbol{A}}_+$, we simply replace $\boldsymbol{D}$ by its nonnegative part $\boldsymbol{D}_+$ to arrive at the rank-$(2k)$ psd approximation

$$\hat{\boldsymbol{A}}_+ := \boldsymbol{\Pi}_{\mathbb{H}_+^n}(\hat{\boldsymbol{A}}) = (\boldsymbol{U}\boldsymbol{V})\boldsymbol{D}_+(\boldsymbol{U}\boldsymbol{V})^*. \tag{6.7}$$

This formula delivers an approximate eigenvalue decomposition of the target matrix.

6.4.3. Algorithm, Costs, and Error. Algorithm 7 contains pseudocode for producing a psd approximation of the form (6.7) from a sketch of the target matrix. As in Algorithm 6, some additional efficiencies are possible

The costs of Algorithm 7 are similar with the symmetric reconstruction method, Algorithm 6. The working storage cost is $\Theta(kn)$, and the arithmetic cost is $\Theta(k\ell n)$.

Combining Theorem 4.1 and Fact 6.1, we obtain a bound on the reconstruction error identical with Corollary 6.2. We omit the details.

7. Fixed-Rank Structured Approximations. Last of all, consider the situation where we need to approximate a structured matrix by a structured matrix with fixed rank. Although the procedures from section 6 produce low-rank approximations, we may require the structured approximation to achieve the target rank r.

As in section 5, we take the most direct approach. We replace an initial structured approximation by the nearest structured matrix with rank r. Projecting a conjugate symmetric (respectively, psd) matrix onto the set of fixed-rank matrices preserves conjugate symmetry (the psd property). The set of matrices with a fixed rank is not convex, however, so the analysis in subsection 6.1 does not apply.

In this section, we present a simple analysis that gives reasonable error bounds for fixed-rank approximations. We also describe algorithms for conjugate symmetric and psd fixed-rank approximation.

7.1. A General Error Bound for Fixed-Rank Approximation. If we have a good initial approximation of the target matrix, we can replace this initial approximation by a fixed-rank matrix without increasing the error significantly. This bound is typically somewhat loose.

PROPOSITION 7.1 (Fixed-Rank Approximation Error). *Let $\boldsymbol{A} \in \mathbb{F}^{m\times n}$ be a target matrix, and let $\hat{\boldsymbol{A}}_{\text{in}} \in \mathbb{F}^{m\times n}$ be an approximation. For any rank parameter r,*

$$\|\boldsymbol{A} - [\![\hat{\boldsymbol{A}}_{\text{in}}]\!]_r\|_{\text{F}} \le \|\boldsymbol{A} - [\![\boldsymbol{A}]\!]_r\|_{\text{F}} + 2\|\boldsymbol{A} - \hat{\boldsymbol{A}}_{\text{in}}\|_{\text{F}}.$$

Proof. Calculate that

$$\begin{aligned}\|\boldsymbol{A} - [\![\hat{\boldsymbol{A}}_{\text{in}}]\!]_r\|_{\text{F}} &\le \|\boldsymbol{A} - \hat{\boldsymbol{A}}_{\text{in}}\|_{\text{F}} + \|\hat{\boldsymbol{A}}_{\text{in}} - [\![\hat{\boldsymbol{A}}_{\text{in}}]\!]_r\|_{\text{F}} \\ &\le \|\boldsymbol{A} - \hat{\boldsymbol{A}}_{\text{in}}\|_{\text{F}} + \|\hat{\boldsymbol{A}}_{\text{in}} - [\![\boldsymbol{A}]\!]_r\|_{\text{F}} \\ &\le 2\|\boldsymbol{A} - \hat{\boldsymbol{A}}_{\text{in}}\|_{\text{F}} + \|\boldsymbol{A} - [\![\boldsymbol{A}]\!]_r\|_{\text{F}}.\end{aligned}$$

The first relation is the triangle inequality. To reach the second line, note that $[\![\hat{\boldsymbol{A}}_{\text{in}}]\!]_r$ is a rank-r approximation of $\hat{\boldsymbol{A}}_{\text{in}}$ with minimal error, while $[\![\boldsymbol{A}]\!]_r$ is an undistinguished rank-r matrix. Last, apply the triangle inequality again. ∎

7.2. Fixed-Rank Conjugate Symmetric Approximation. Assume that the target matrix $\boldsymbol{A} \in \mathbb{H}^n$ is conjugate symmetric and we wish to compute a rank-r conjugate symmetric approximation. First, form an initial approximation $\hat{\boldsymbol{A}}_{\text{sym}}$ using the procedure (6.6) in subsection 6.3.2. Then compute an r-truncated eigenvalue decomposition of the matrix $\boldsymbol{S}$ defined in (6.5):

$$\boldsymbol{S} =: \boldsymbol{V}[\![\boldsymbol{D}]\!]_r\boldsymbol{V}^* \;+\; \text{approximation error}.$$

In view of the representation (6.6),

$$[\![\hat{\boldsymbol{A}}_{\text{sym}}]\!]_r = (\boldsymbol{U}\boldsymbol{V})[\![\boldsymbol{D}]\!]_r(\boldsymbol{U}\boldsymbol{V})^*. \tag{7.1}$$

Algorithm 8 contains pseudocode for the fixed-rank approximation (7.1). The total working storage is $\Theta(kn)$, and the arithmetic cost is $\Theta(k\ell n)$. Corollary 6.2 and Proposition 7.1 yield the following error bound.

COROLLARY 7.2 (Fixed-Rank Symmetric Reconstruction). *Assume that the target matrix $\boldsymbol{A} \in \mathbb{H}^n(\mathbb{F})$ is conjugate symmetric, and assume that the sketch size parameters satisfy $k > r + \alpha$ and $\ell > k + \alpha$. Draw random test matrices $\boldsymbol{\Omega} \in \mathbb{F}^{n\times k}$*

Algorithm 8 *Single-View Fixed-Rank Symmetric Approximation.* Implements (7.1).

Require: Matrix dimensions $m = n$; target rank $r \le k$
Ensure: Returns factors $\boldsymbol{U} \in \mathbb{F}^{n\times r}$ with orthonormal columns and diagonal $\boldsymbol{D} \in \mathbb{H}^r$ that form a rank-r conjugate symmetric approximation $\hat{\boldsymbol{A}}_{\text{out}} = \boldsymbol{U}\boldsymbol{D}\boldsymbol{U}^*$ of the sketched matrix

function SKETCH.FIXEDRANKSYMAPPROX(r)
  $(\boldsymbol{U}, \boldsymbol{S}) \leftarrow$ LOWRANKSYMAPPROX( ) ▷ Get $\hat{\boldsymbol{A}}_{\text{in}} = \boldsymbol{U}\boldsymbol{S}\boldsymbol{U}^*$
  $(\boldsymbol{V}, \boldsymbol{D}) \leftarrow \texttt{eigs}(\boldsymbol{S}, r, \texttt{'lm'})$ ▷ Truncate full eigendecomposition
  $\boldsymbol{U} \leftarrow \boldsymbol{U}\boldsymbol{V}$ ▷ Consolidate orthonormal factors
  return $(\boldsymbol{U}, \boldsymbol{D})$

Algorithm 9 *Single-View Fixed-Rank PSD Approximation.* Implements (7.2).

Require: Matrix dimensions $m = n$; target rank $r \le k$
Ensure: Returns factors $\boldsymbol{U} \in \mathbb{F}^{n\times r}$ with orthonormal columns and nonnegative, diagonal $\boldsymbol{D} \in \mathbb{H}^r_+$ that form a rank-r psd approximation $\hat{\boldsymbol{A}}_{\text{out}} = \boldsymbol{U}\boldsymbol{D}\boldsymbol{U}^*$ of the sketched matrix

function SKETCH.FIXEDRANKPSDAPPROX(r)
  $(\boldsymbol{U}, \boldsymbol{S}) \leftarrow$ LOWRANKSYMAPPROX( ) ▷ Get $\hat{\boldsymbol{A}}_{\text{in}} = \boldsymbol{U}\boldsymbol{S}\boldsymbol{U}^*$
  $(\boldsymbol{V}, \boldsymbol{D}) \leftarrow \texttt{eigs}(\boldsymbol{S}, r, \texttt{'lr'})$ ▷ Truncate full eigendecomposition
  $\boldsymbol{U} \leftarrow \boldsymbol{U}\boldsymbol{V}$ ▷ Consolidate orthonormal factors
  $\boldsymbol{D} \leftarrow \texttt{max}(\boldsymbol{D}, 0)$ ▷ Zero out negative eigenvalues
  return $(\boldsymbol{U}, \boldsymbol{D})$

and $\boldsymbol{\Psi} \in \mathbb{F}^{\ell\times n}$ independently from the standard normal distribution. Then the rank-r conjugate symmetric approximation $[\![\hat{\boldsymbol{A}}_{\text{sym}}]\!]_r$ produced by (7.1) satisfies

$$\mathbb{E}\,\|\boldsymbol{A} - [\![\hat{\boldsymbol{A}}_{\text{sym}}]\!]_r\|_{\text{F}} \le \left[1 + 2\sqrt{(1 + f(r,k))(1 + f(k,\ell))}\right] \cdot \|\boldsymbol{A} - [\![\boldsymbol{A}]\!]_r\|_{\text{F}}.$$

The function f is defined in (4.5), and the number α is given by (2.1).

7.3. Fixed-Rank PSD Approximation. Assume that the target matrix $\boldsymbol{A} \in \mathbb{H}^n_+$ is psd, and we wish to compute a rank-r psd approximation $[\![\hat{\boldsymbol{A}}_+]\!]_r$. First, form an initial approximation $\hat{\boldsymbol{A}}_+$ using the procedure (6.7) in subsection 6.4.2. Then compute an r-truncated positive eigenvalue decomposition of the matrix $\boldsymbol{S}$ defined in (6.5):

$$\boldsymbol{S} =: \boldsymbol{V}[\![\boldsymbol{D}_+]\!]_r\boldsymbol{V}^* \;+\; \text{approximation error}.$$

In view of the representation (6.7),

$$[\![\hat{\boldsymbol{A}}_+]\!]_r = (\boldsymbol{U}\boldsymbol{V})[\![\boldsymbol{D}_+]\!]_r(\boldsymbol{U}\boldsymbol{V})^*. \tag{7.2}$$

Algorithm 9 contains pseudocode for the fixed-rank psd approximation (7.2). The working storage is $\Theta(kn)$, and the arithmetic cost is $\Theta(k\ell n)$. Corollary 6.2 and Proposition 7.1 produce an error bound identical with Corollary 7.2; we omit the details.

8. Analysis of Low-Rank Approximation. In this section, we develop theoretical results on the performance of the basic low-rank approximation (4.3) implemented in Algorithms 3 and 4.

8.1. Facts about Random Matrices. Our arguments require classical formulae for the expectations of functions of a standard normal matrix. In the real case, these results are [14, Prop. A.1 and A.6]. The complex case follows from the same principles, so we omit the details.

FACT 8.1. *Let $\boldsymbol{G} \in \mathbb{F}^{t\times s}$ be a standard normal matrix. For all matrices $\boldsymbol{B}$ and $\boldsymbol{C}$ with conforming dimensions,*

$$\mathbb{E}\,\|\boldsymbol{BGC}\|_{\mathrm{F}}^2 = \beta\|\boldsymbol{B}\|_{\mathrm{F}}^2\|\boldsymbol{C}\|_{\mathrm{F}}^2. \tag{8.1}$$

Furthermore, if $t > s + \alpha$,

$$\mathbb{E}\,\|\boldsymbol{G}^\dagger\|_{\mathrm{F}}^2 = \frac{1}{\beta}\cdot\frac{s}{t-s-\alpha} = \frac{1}{\beta}\cdot f(s,t). \tag{8.2}$$

The function f is introduced in (4.5), and the numbers α and β are given by (2.1).

We also need results [14, Prop. A.2 and A.4] on the expected spectral norm of some functions of a standard normal matrix. Note that we only present these facts in the real setting.

FACT 8.2. *Let $\boldsymbol{G} \in \mathbb{R}^{t\times s}$ be a real standard normal matrix. For all matrices $\boldsymbol{B}$ and $\boldsymbol{C}$ with conforming dimensions,*

$$\mathbb{E}\,\|\boldsymbol{BGC}\| \le \|\boldsymbol{B}\|_{\mathrm{F}}\|\boldsymbol{C}\| + \|\boldsymbol{B}\|\|\boldsymbol{C}\|_{\mathrm{F}}. \tag{8.3}$$

Furthermore, if $t > s$,

$$\mathbb{E}\,\|\boldsymbol{G}^\dagger\| \le \frac{\mathrm{e}\sqrt{t}}{t-s} = h(s,t). \tag{8.4}$$

The function h also appears in (4.7).

8.2. Results from Randomized Linear Algebra. Our arguments also depend heavily on the analysis of randomized low-rank approximation developed in [14, Sec. 10]. We state these results using the familiar notation from sections 3 and 4.

FACT 8.3 (Halko et al. 2011). *Fix $\boldsymbol{A} \in \mathbb{F}^{m\times n}$. Assume that $k > r + \alpha$. Draw the random test matrix $\boldsymbol{\Omega} \in \mathbb{F}^{k\times n}$ from the standard normal distribution. Then the matrix $\boldsymbol{Q}$ computed by (4.1) satisfies*

$$\mathbb{E}_{\boldsymbol{\Omega}}\,\|\boldsymbol{A} - \boldsymbol{QQ}^*\boldsymbol{A}\|_{\mathrm{F}}^2 \le (1 + f(r,k))\cdot\|\boldsymbol{A} - [\![\boldsymbol{A}]\!]_r\|_{\mathrm{F}}^2.$$

The function f is introduced in (4.5), and the number α is given by (2.1).

This result follows immediately from the proof of [14, Thm. 10.5] using Fact 8.1 to handle both the real and complex case simultaneously.

We also require a spectral-norm error bound derived in [14, Sec. 10]. Note that this result is only given for the real case.

FACT 8.4 (Halko et al. 2011). *Fix $\boldsymbol{A} \in \mathbb{R}^{m\times n}$. Assume that $k > r+1$. Draw the random test matrix $\boldsymbol{\Omega} \in \mathbb{R}^{k\times n}$ from the real standard normal distribution. Then the matrix $\boldsymbol{Q}$ computed by (4.1) satisfies*

$$\mathbb{E}_{\boldsymbol{\Omega}}\,\|\boldsymbol{A} - \boldsymbol{QQ}^*\boldsymbol{A}\| \le g(r,k)\cdot\|\boldsymbol{A} - [\![\boldsymbol{A}]\!]_r\| + h(r,k)\cdot\|\boldsymbol{A} - [\![\boldsymbol{A}]\!]_r\|_{\mathrm{F}}.$$

The functions g and h are defined in (4.7).

8.3. Proof of Theorem 4.1: Frobenius Error Bound. In this section, we establish the Frobenius-norm error bound for the low-rank approximation (4.3). We maintain the notation from sections 3 and 4, and we state explicitly when we are making distributional assumptions on the test matrices.

8.3.1. Decomposition of the Approximation Error. Fact 8.3 formalizes the intuition that $\boldsymbol{A} \approx \boldsymbol{Q}(\boldsymbol{Q}^*\boldsymbol{A})$. The main object of the proof is to demonstrate that $\boldsymbol{X} \approx \boldsymbol{Q}^*\boldsymbol{A}$. The first step in the argument is to break down the approximation error into these two parts.

LEMMA 8.5. *The approximation error decomposes as*

$$\|\boldsymbol{A} - \hat{\boldsymbol{A}}\|_{\mathrm{F}}^2 = \|\boldsymbol{A} - \boldsymbol{Q}\boldsymbol{Q}^*\boldsymbol{A}\|_{\mathrm{F}}^2 + \|\boldsymbol{X} - \boldsymbol{Q}^*\boldsymbol{A}\|_{\mathrm{F}}^2.$$

Proof. Recall that $\hat{\boldsymbol{A}} = \boldsymbol{Q}\boldsymbol{X}$, and calculate that

$$\begin{aligned}\|\boldsymbol{A} - \boldsymbol{Q}\boldsymbol{X}\|_{\mathrm{F}}^2 &= \|(\mathbf{I} - \boldsymbol{Q}\boldsymbol{Q}^*)\boldsymbol{A} + \boldsymbol{Q}(\boldsymbol{Q}^*\boldsymbol{A} - \boldsymbol{X})\|_{\mathrm{F}}^2 \\ &= \|(\mathbf{I} - \boldsymbol{Q}\boldsymbol{Q}^*)\boldsymbol{A}\|_{\mathrm{F}}^2 + \|\boldsymbol{Q}(\boldsymbol{Q}^*\boldsymbol{A} - \boldsymbol{X})\|_{\mathrm{F}}^2 \\ &= \|\boldsymbol{A} - \boldsymbol{Q}\boldsymbol{Q}^*\boldsymbol{A}\|_{\mathrm{F}}^2 + \|\boldsymbol{Q}^*\boldsymbol{A} - \boldsymbol{X}\|_{\mathrm{F}}^2.\end{aligned}$$

The second line follows from the Pythagorean theorem, which is valid because the ranges of $\mathbf{I} - \boldsymbol{Q}\boldsymbol{Q}^*$ and $\boldsymbol{Q}$ are orthogonal. The last identity holds because $\boldsymbol{Q}$ has orthonormal columns and the Frobenius norm is unitarily invariant. ∎

8.3.2. Approximating the Second Factor. Next, we develop an explicit expression for the error in the approximation $\boldsymbol{X} \approx \boldsymbol{Q}^*\boldsymbol{A}$. It is convenient to construct a matrix $\boldsymbol{P} \in \mathbb{F}^{n\times(n-k)}$ with orthonormal columns that satisfies

$$\boldsymbol{P}\boldsymbol{P}^* = \mathbf{I} - \boldsymbol{Q}\boldsymbol{Q}^*. \tag{8.5}$$

Introduce the matrices

$$\boldsymbol{\Psi}_1 := \boldsymbol{\Psi}\boldsymbol{P} \in \mathbb{F}^{\ell\times(n-k)} \quad \text{and} \quad \boldsymbol{\Psi}_2 := \boldsymbol{\Psi}\boldsymbol{Q} \in \mathbb{F}^{\ell\times k}. \tag{8.6}$$

We are now prepared to state the result.

LEMMA 8.6. *Assume that the matrix $\boldsymbol{\Psi}_2$ has full column-rank. Then*

$$\boldsymbol{X} - \boldsymbol{Q}^*\boldsymbol{A} = \boldsymbol{\Psi}_2^\dagger\boldsymbol{\Psi}_1(\boldsymbol{P}^*\boldsymbol{A}). \tag{8.7}$$

The matrices $\boldsymbol{\Psi}_1$ and $\boldsymbol{\Psi}_2$ are defined in (8.6).

Proof. Recall that $\boldsymbol{W} = \boldsymbol{\Psi}\boldsymbol{A}$, and calculate that

$$\boldsymbol{W} = \boldsymbol{\Psi}\boldsymbol{A} = \boldsymbol{\Psi}\boldsymbol{P}\boldsymbol{P}^*\boldsymbol{A} + \boldsymbol{\Psi}\boldsymbol{Q}\boldsymbol{Q}^*\boldsymbol{A} = \boldsymbol{\Psi}_1(\boldsymbol{P}^*\boldsymbol{A}) + \boldsymbol{\Psi}_2(\boldsymbol{Q}^*\boldsymbol{A}).$$

The second relation holds because $\boldsymbol{P}\boldsymbol{P}^* + \boldsymbol{Q}\boldsymbol{Q}^* = \mathbf{I}$. Then we use (8.6) to identify $\boldsymbol{\Psi}_1$ and $\boldsymbol{\Psi}_2$. By hypothesis, the matrix $\boldsymbol{\Psi}_2$ has full column-rank, so we can left-multiply the last display by $\boldsymbol{\Psi}_2^\dagger$ to attain

$$\boldsymbol{\Psi}_2^\dagger\boldsymbol{W} = \boldsymbol{\Psi}_2^\dagger\boldsymbol{\Psi}_1(\boldsymbol{P}^*\boldsymbol{A}) + \boldsymbol{Q}^*\boldsymbol{A}.$$

Turning back to (4.2), we identify $\boldsymbol{X} = \boldsymbol{\Psi}_2^\dagger\boldsymbol{W}$. ∎

8.3.3. The Expected Frobenius-Norm Error in the Second Factor. We are now prepared to compute the average Frobenius-norm error in approximating $\boldsymbol{Q}^*\boldsymbol{A}$ by means of the matrix $\boldsymbol{X}$. In contrast to the previous steps, this part of the argument relies on distributional assumptions on the test matrix $\boldsymbol{\Psi}$. Remarkably, for a Gaussian test matrix, $\boldsymbol{X}$ is even an unbiased estimator of the factor $\boldsymbol{Q}^*\boldsymbol{A}$.

LEMMA 8.7. *Assume that $\boldsymbol{\Psi} \in \mathbb{F}^{\ell\times n}$ is a standard normal matrix that is independent from $\boldsymbol{\Omega}$. Then*

$$\mathbb{E}_{\boldsymbol{\Psi}}[\boldsymbol{X} - \boldsymbol{Q}^*\boldsymbol{A}] = \mathbf{0}.$$

Furthermore,

$$\mathbb{E}_{\boldsymbol{\Psi}} \|\boldsymbol{X} - \boldsymbol{Q}^*\boldsymbol{A}\|_{\mathrm{F}}^2 = f(k,\ell) \cdot \|\boldsymbol{A} - \boldsymbol{Q}\boldsymbol{Q}^*\boldsymbol{A}\|_{\mathrm{F}}^2.$$

Proof. Observe that $\boldsymbol{P}$ and $\boldsymbol{Q}$ are partial isometries with orthogonal ranges. Owing to the marginal property of the standard normal distribution, the random matrices $\boldsymbol{\Psi}_1$ and $\boldsymbol{\Psi}_2$ are statistically independent standard normal matrices. In particular, $\boldsymbol{\Psi}_2 \in \mathbb{F}^{\ell\times k}$ almost surely has full column-rank because the assumption (3.1) requires that $\ell \geq k$.

First, take the expectation of the identity (8.7) to see that

$$\mathbb{E}_{\boldsymbol{\Psi}}[\boldsymbol{X} - \boldsymbol{Q}^*\boldsymbol{A}] = \mathbb{E}_{\boldsymbol{\Psi}_2}\, \mathbb{E}_{\boldsymbol{\Psi}_1}[\boldsymbol{\Psi}_2^\dagger \boldsymbol{\Psi}_1 \boldsymbol{P}^*\boldsymbol{A}] = \mathbf{0}.$$

In the first relation, we use the statistical independence of $\boldsymbol{\Psi}_1$ and $\boldsymbol{\Psi}_2$ to write the expectation as an iterated expectation. Then we observe that $\boldsymbol{\Psi}_1$ is a matrix with zero mean.

Next, take the expected squared Frobenius norm of (8.7) to see that

$$\begin{aligned}\mathbb{E}_{\boldsymbol{\Psi}} \|\boldsymbol{X} - \boldsymbol{Q}^*\boldsymbol{A}\|_{\mathrm{F}}^2 &= \mathbb{E}_{\boldsymbol{\Psi}_2}\, \mathbb{E}_{\boldsymbol{\Psi}_1} \|\boldsymbol{\Psi}_2^\dagger \boldsymbol{\Psi}_1 (\boldsymbol{P}^*\boldsymbol{A})\|_{\mathrm{F}}^2 \\ &= \beta \cdot \mathbb{E}_{\boldsymbol{\Psi}_2} \left[\|\boldsymbol{\Psi}_2^\dagger\|_{\mathrm{F}}^2 \cdot \|\boldsymbol{P}^*\boldsymbol{A}\|_{\mathrm{F}}^2\right] = f(k,\ell) \cdot \|\boldsymbol{P}^*\boldsymbol{A}\|_{\mathrm{F}}^2.\end{aligned}$$

The last two identities follow from (8.1) and (8.2) respectively, where we use the fact that $\boldsymbol{\Psi}_2 \in \mathbb{F}^{\ell\times k}$. To conclude, note that

$$\|\boldsymbol{P}^*\boldsymbol{A}\|_{\mathrm{F}}^2 = \|\boldsymbol{P}\boldsymbol{P}^*\boldsymbol{A}\|_{\mathrm{F}}^2 = \|\boldsymbol{A} - \boldsymbol{Q}\boldsymbol{Q}^*\boldsymbol{A}\|_{\mathrm{F}}^2.$$

The first relation holds because $\boldsymbol{P}$ is a partial isometry and the Frobenius norm is unitarily invariant. Last, we apply the definition (8.5) of $\boldsymbol{P}$. ∎

8.3.4. Proof of Theorem 4.1. We are now prepared to complete the proof of the Frobenius-norm error bound stated in Theorem 4.1. For this argument, we assume that the test matrices $\boldsymbol{\Omega} \in \mathbb{F}^{n\times k}$ and $\boldsymbol{\Psi} \in \mathbb{F}^{\ell\times m}$ are drawn independently from the standard normal distribution.

According to Lemma 8.5,

$$\|\boldsymbol{A} - \hat{\boldsymbol{A}}\|_{\mathrm{F}}^2 = \|\boldsymbol{A} - \boldsymbol{Q}\boldsymbol{Q}^*\boldsymbol{A}\|_{\mathrm{F}}^2 + \|\boldsymbol{X} - \boldsymbol{Q}^*\boldsymbol{A}\|_{\mathrm{F}}^2.$$

Take the expectation of the last display to reach

$$\begin{aligned}\mathbb{E}\, \|\boldsymbol{A} - \hat{\boldsymbol{A}}\|_{\mathrm{F}}^2 &= \mathbb{E}_{\boldsymbol{\Omega}} \|\boldsymbol{A} - \boldsymbol{Q}\boldsymbol{Q}^*\boldsymbol{A}\|_{\mathrm{F}}^2 + \mathbb{E}_{\boldsymbol{\Omega}}\, \mathbb{E}_{\boldsymbol{\Psi}} \|\boldsymbol{X} - \boldsymbol{Q}^*\boldsymbol{A}\|_{\mathrm{F}}^2 \\ &= (1 + f(k,\ell)) \cdot \mathbb{E}_{\boldsymbol{\Omega}} \|\boldsymbol{A} - \boldsymbol{Q}\boldsymbol{Q}^*\boldsymbol{A}\|_{\mathrm{F}}^2 \\ &\leq (1 + f(k,\ell))(1 + f(r,k)) \cdot \|\boldsymbol{A} - [\![\boldsymbol{A}]\!]_r\|_{\mathrm{F}}^2.\end{aligned}$$

In the first line, we use the independence of the two random matrices to write the expectation as an iterated expectation. To reach the second line, we apply Lemma 8.7 to the second term. Finally, we invoke the randomized linear algebra result, Fact 8.3.

8.4. Proof of Theorem 4.2: Spectral Error Bound. In this section, we establish a spectral-norm error bound for the low-rank approximation (4.3). We continue to use the notation from sections 3 and 4, and we emphasize that we are now working in the real setting. As similar result holds true in the complex setting, but facts about complex standard normal matrices were not immediately available.

8.4.1. Decomposition of the Approximation Error. As before, the first step in the argument is to break down the error as $\boldsymbol{A} \approx \boldsymbol{Q}(\boldsymbol{Q}^*\boldsymbol{A})$ and $\boldsymbol{X} \approx \boldsymbol{Q}^*\boldsymbol{A}$.

LEMMA 8.8. *The approximation error decomposes as*

$$\|\boldsymbol{A} - \hat{\boldsymbol{A}}\| \le \|\boldsymbol{A} - \boldsymbol{Q}\boldsymbol{Q}^*\boldsymbol{A}\| + \|\boldsymbol{X} - \boldsymbol{Q}^*\boldsymbol{A}\|$$

Proof. Recall that $\hat{\boldsymbol{A}} = \boldsymbol{Q}\boldsymbol{X}$, and observe that

$$\begin{aligned}\|\boldsymbol{A} - \boldsymbol{Q}\boldsymbol{X}\| &\le \|\boldsymbol{A} - \boldsymbol{Q}\boldsymbol{Q}^*\boldsymbol{A}\| + \|\boldsymbol{Q}(\boldsymbol{Q}^*\boldsymbol{A} - \boldsymbol{X})\| \\ &= \|\boldsymbol{A} - \boldsymbol{Q}\boldsymbol{Q}^*\boldsymbol{A}\| + \|\boldsymbol{Q}^*\boldsymbol{A} - \boldsymbol{X}\|.\end{aligned}$$

The first relation is the triangle inequality, and the second holds because $\boldsymbol{Q}$ has orthonormal columns and the spectral norm is unitarily invariant. ∎

8.4.2. The Expected Spectral-Norm Error in the Second Factor. Next, we bound the spectral-norm error in approximating $\boldsymbol{Q}^*\boldsymbol{A}$ by $\boldsymbol{X}$. This argument relies on distributional assumptions on the test matrix $\boldsymbol{\Psi}$.

LEMMA 8.9. *Assume that $\boldsymbol{\Psi} \in \mathbb{R}^{\ell\times n}$ is a real standard normal matrix that is independent from $\boldsymbol{\Omega}$. Then*

$$\mathbb{E}_{\boldsymbol{\Psi}} \|\boldsymbol{X} - \boldsymbol{Q}^*\boldsymbol{A}\| \le \sqrt{f(k,\ell)} \cdot \|\boldsymbol{A} - \boldsymbol{Q}\boldsymbol{Q}^*\boldsymbol{A}\| + h(k,\ell) \cdot \|\boldsymbol{A} - \boldsymbol{Q}\boldsymbol{Q}^*\boldsymbol{A}\|_{\mathrm{F}}.$$

The functions f and h are defined in (4.5) and (4.7).

Proof. The proof is similar with the proof of Lemma 8.7, but we also use Fact 8.2 to bound expectations. The expected spectral norm of the identity (8.7) satisfies

$$\begin{aligned}\mathbb{E}_{\boldsymbol{\Psi}} \|\boldsymbol{X} - \boldsymbol{Q}^*\boldsymbol{A}\| &= \mathbb{E}_{\boldsymbol{\Psi}_2} \mathbb{E}_{\boldsymbol{\Psi}_1} \|\boldsymbol{\Psi}_2^\dagger \boldsymbol{\Psi}_1(\boldsymbol{P}^*\boldsymbol{A})\| \\ &= \mathbb{E}_{\boldsymbol{\Psi}_2} \left[\|\boldsymbol{\Psi}_2^\dagger\|_{\mathrm{F}} \cdot \|\boldsymbol{P}^*\boldsymbol{A}\| + \|\boldsymbol{\Psi}_2^\dagger\| \|\boldsymbol{P}^*\boldsymbol{A}\|_{\mathrm{F}}\right] \\ &\le \sqrt{f(k,\ell)} \cdot \|\boldsymbol{P}^*\boldsymbol{A}\| + h(k,\ell) \cdot \|\boldsymbol{P}^*\boldsymbol{A}\|_{\mathrm{F}}.\end{aligned}$$

The second line follows from (8.3), while the last line depends on (8.2) and (8.4). Finally, use the definition (8.5) of $\boldsymbol{P}$ to rewrite the norms of $\boldsymbol{P}^*\boldsymbol{A}$ in terms of $\boldsymbol{Q}$. ∎

8.4.3. Proof of Theorem 4.2. We may now complete the proof of the spectral-norm error bound stated in Theorem 4.2. Assume that the test matrices $\boldsymbol{\Omega} \in \mathbb{R}^{n\times k}$ and $\boldsymbol{\Psi} \in \mathbb{R}^{\ell\times m}$ are drawn independently from the real standard normal distribution.

According to Lemma 8.8,

$$\|\boldsymbol{A} - \hat{\boldsymbol{A}}\| \le \|\boldsymbol{A} - \boldsymbol{Q}\boldsymbol{Q}^*\boldsymbol{A}\| + \|\boldsymbol{X} - \boldsymbol{Q}^*\boldsymbol{A}\|.$$

Take the expectation of the last display to reach

$$\begin{aligned}\mathbb{E}\,\|\boldsymbol{A} - \hat{\boldsymbol{A}}\| &\le \mathbb{E}_{\boldsymbol{\Omega}} \|\boldsymbol{A} - \boldsymbol{Q}\boldsymbol{Q}^*\boldsymbol{A}\| + \mathbb{E}_{\boldsymbol{\Omega}} \mathbb{E}_{\boldsymbol{\Psi}} \|\boldsymbol{X} - \boldsymbol{Q}^*\boldsymbol{A}\| \\ &\le \left(1 + \sqrt{f(k,\ell)}\right) \cdot \mathbb{E}_{\boldsymbol{\Omega}} \|\boldsymbol{A} - \boldsymbol{Q}\boldsymbol{Q}^*\boldsymbol{A}\| + h(k,\ell) \cdot \mathbb{E}_{\boldsymbol{\Omega}} \|\boldsymbol{A} - \boldsymbol{Q}\boldsymbol{Q}^*\boldsymbol{A}\|_{\mathrm{F}} \\ &= g(k,\ell) \cdot \mathbb{E}_{\boldsymbol{\Omega}} \|\boldsymbol{A} - \boldsymbol{Q}\boldsymbol{Q}^*\boldsymbol{A}\| + h(k,\ell) \cdot \mathbb{E}_{\boldsymbol{\Omega}} \|\boldsymbol{A} - \boldsymbol{Q}\boldsymbol{Q}^*\boldsymbol{A}\|_{\mathrm{F}}.\end{aligned}$$

The second inequality follows from Lemma 8.9, and then we identify the function g from (4.7). Invoke Facts 8.3 and 8.4, and rearrange to arrive at the bound

$$\begin{aligned}\mathbb{E}\,\|\boldsymbol{A} - \hat{\boldsymbol{A}}\| &\le g(r,k)\cdot g(k,\ell)\cdot\|\boldsymbol{A} - [\![\boldsymbol{A}]\!]_r\| \\ &\quad + \big[h(r,k)\cdot g(k,\ell) + g(r,k)\cdot h(k,\ell)\big]\cdot\|\boldsymbol{A} - [\![\boldsymbol{A}]\!]_r\|_{\mathrm{F}}.\end{aligned}$$

This is the stated result.

9. Analysis of Fixed-Rank Approximation. In this section, we develop an analysis of the fixed-rank approximation scheme (5.2) that is implemented in Algorithm 5. We maintain the notation from sections 3 and 4. We state explicitly when we are making distributional assumptions on the test matrices.

9.1. Facts from (Randomized) Linear Algebra. First, we require a variational principle obtained in [13, Thm. 3.5].

FACT 9.1 (Gu [13]). *Let $\boldsymbol{M} \in \mathbb{F}^{m\times n}$ be an arbitrary matrix, and let $\boldsymbol{U} \in \mathbb{F}^{m\times k}$ be a matrix with orthonormal columns. For any rank parameter r,*

$$\min_{\operatorname{rank}\boldsymbol{Z}\le r} \|\boldsymbol{M} - \boldsymbol{U}\boldsymbol{Z}\|_{\mathrm{F}}^2 = \|\boldsymbol{M} - \boldsymbol{U}[\![\boldsymbol{U}^*\boldsymbol{M}]\!]_r\|_{\mathrm{F}}^2.$$

Our argument also relies on a new result about randomized matrix approximation.

PROPOSITION 9.2. *Assume that $k > r + \alpha$. Draw the random test matrix $\boldsymbol{\Omega} \in \mathbb{F}^{k\times n}$ from the standard normal distribution. Then the matrix $\boldsymbol{Q}$ computed by (4.1) satisfies*

$$\mathbb{E}_{\boldsymbol{\Omega}}\,\|\boldsymbol{A} - \boldsymbol{Q}\boldsymbol{Q}^*[\![\boldsymbol{A}]\!]_r\|_{\mathrm{F}}^2 \le (1 + f(r,k))\cdot\|\boldsymbol{A} - [\![\boldsymbol{A}]\!]_r\|_{\mathrm{F}}^2.$$

The function f is defined in (4.5), and the number α is given by (2.1).

This result is a subtle variant on Fact 8.3. The proof is based on the same principles, but a detailed account would require us to repeat a significant part of the presentation in [14, Sec. 9]. We include only a summary.

Proof Sketch. First, observe that

$$\|\boldsymbol{A} - \boldsymbol{Q}\boldsymbol{Q}^*[\![\boldsymbol{A}]\!]_r\|_{\mathrm{F}}^2 = \|\boldsymbol{A} - [\![\boldsymbol{A}]\!]_r\|_{\mathrm{F}}^2 + \|(\mathbf{I} - \boldsymbol{Q}\boldsymbol{Q}^*)[\![\boldsymbol{A}]\!]_r\|_{\mathrm{F}}^2.$$

For example, see [13, Thm. 3.5]. To bound the second term, we write the partitioned SVD of the matrix $\boldsymbol{A}$ as

$$\boldsymbol{A} = \boldsymbol{U}\begin{bmatrix}\boldsymbol{\Sigma}_1 & \\ & \boldsymbol{\Sigma}_2\end{bmatrix}\begin{bmatrix}\boldsymbol{V}_1^* \\ \boldsymbol{V}_2^*\end{bmatrix}$$

where $\boldsymbol{\Sigma}_1 \in \mathbb{F}^{r\times r}$ and the singular values are arranged in weakly decreasing order. We also introduce the matrices $\boldsymbol{\Omega}_1 := \boldsymbol{V}_1^*\boldsymbol{\Omega}$ and $\boldsymbol{\Omega}_2 := \boldsymbol{V}_2^*\boldsymbol{\Omega}$. In the proof of [14, Thm. 9.1], we simply replace the matrix $\boldsymbol{A}$ with the matrix $[\![\boldsymbol{A}]\!]_r$ to obtain the bound

$$\|(\mathbf{I} - \boldsymbol{Q}\boldsymbol{Q}^*)[\![\boldsymbol{A}]\!]_r\|_{\mathrm{F}}^2 \le \|\boldsymbol{\Sigma}_2\boldsymbol{\Omega}_2\boldsymbol{\Omega}_1^{\dagger}\|_{\mathrm{F}}^2.$$

[The additional term in [14, Thm. 9.1] derives from the $(r+1)$th and smaller singular values of $\boldsymbol{A}$; for the matrix $[\![\boldsymbol{A}]\!]_r$, it vanishes because the corresponding singular values are zero.] As in the proof of Lemma 8.7 or in the proof of [14, Thm. 10.5], we have

$$\mathbb{E}\,\|\boldsymbol{\Sigma}_2\boldsymbol{\Omega}_2\boldsymbol{\Omega}_1^{\dagger}\|_{\mathrm{F}}^2 = f(k,\ell)\cdot\|\boldsymbol{\Sigma}_2\|_{\mathrm{F}}^2 = f(k,\ell)\cdot\|\boldsymbol{A} - [\![\boldsymbol{A}]\!]_r\|_{\mathrm{F}}^2.$$

In the last step, we have noticed that $\|\boldsymbol{\Sigma}_2\|_{\mathrm{F}}^2 = \|\boldsymbol{A} - [\![\boldsymbol{A}]\!]_r\|_{\mathrm{F}}^2$. ∎

9.2. Proof of Theorem 5.1. Assume that the test matrices $\boldsymbol{\Omega} \in \mathbb{F}^{n\times k}$ and $\boldsymbol{\Psi} \in \mathbb{F}^{\ell\times m}$ are drawn independently from the standard normal distribution. Recall from (5.2) that our rank-r approximation takes the form $[\![\hat{\boldsymbol{A}}]\!]_r = \boldsymbol{Q}[\![\boldsymbol{X}]\!]_r$. According to Lemma 8.6,

$$\boldsymbol{X} = \boldsymbol{Q}^*\boldsymbol{A} + \boldsymbol{E} \quad \text{where} \quad \boldsymbol{E} := \boldsymbol{\Psi}_2^\dagger \boldsymbol{\Psi}_1(\boldsymbol{P}^*\boldsymbol{A}). \tag{9.1}$$

We develop a perturbation argument to show that the error term $\boldsymbol{E}$ has a limited effect on the fixed-rank approximation.

We can make the deterministic calculation

$$\begin{aligned}
\|\boldsymbol{A} - [\![\hat{\boldsymbol{A}}]\!]_r\|_{\mathrm{F}} &= \|\boldsymbol{A} - \boldsymbol{Q}[\![\boldsymbol{Q}^*\boldsymbol{A} + \boldsymbol{E}]\!]_r\|_{\mathrm{F}} \\
&\le \|(\boldsymbol{A} + \boldsymbol{Q}\boldsymbol{E}) - \boldsymbol{Q}[\![\boldsymbol{Q}^*\boldsymbol{A} + \boldsymbol{E}]\!]_r\|_{\mathrm{F}} + \|\boldsymbol{Q}\boldsymbol{E}\|_{\mathrm{F}} \\
&\le \|(\boldsymbol{A} + \boldsymbol{Q}\boldsymbol{E}) - \boldsymbol{Q}(\boldsymbol{Q}^*[\![\boldsymbol{A}]\!]_r)\|_{\mathrm{F}} + \|\boldsymbol{Q}\boldsymbol{E}\|_{\mathrm{F}} \\
&\le \|\boldsymbol{A} - \boldsymbol{Q}\boldsymbol{Q}^*[\![\boldsymbol{A}]\!]_r\|_{\mathrm{F}} + 2\|\boldsymbol{Q}\boldsymbol{E}\|_{\mathrm{F}} \\
&= \|\boldsymbol{A} - \boldsymbol{Q}\boldsymbol{Q}^*[\![\boldsymbol{A}]\!]_r\|_{\mathrm{F}} + 2\|\boldsymbol{\Psi}_2^\dagger\boldsymbol{\Psi}_1(\boldsymbol{P}^*\boldsymbol{A})\|_{\mathrm{F}}.
\end{aligned}$$

In the second line, we applied the triangle inequality. When $\boldsymbol{M} = \boldsymbol{A} + \boldsymbol{Q}\boldsymbol{E}$ and $\boldsymbol{U} = \boldsymbol{Q}$, the rank-$r$ matrix $[\![\boldsymbol{Q}^*(\boldsymbol{A} + \boldsymbol{Q}\boldsymbol{E})]\!]_r = [\![\boldsymbol{Q}^*\boldsymbol{A} + \boldsymbol{E}]\!]_r$ is a minimizer of the variational problem from Fact 9.1. To reach the next line, we replace this minimizer with the undistinguished rank-r matrix $\boldsymbol{Q}^*[\![\boldsymbol{A}]\!]_r$. The penultimate line follows from the triangle inequality. Last, we use unitary invariance to remove $\boldsymbol{Q}$ from the second term, and we recall the definition (9.1) of $\boldsymbol{E}$.

Take the expectation of the previous display to arrive at

$$\begin{aligned}
\mathbb{E}\,\|\boldsymbol{A} - [\![\hat{\boldsymbol{A}}]\!]_r\|_{\mathrm{F}} &\le \left(\mathbb{E}_{\boldsymbol{\Omega}}\,\|\boldsymbol{A} - \boldsymbol{Q}\boldsymbol{Q}^*[\![\boldsymbol{A}]\!]_r\|_{\mathrm{F}}^2\right)^{1/2} + 2\left(\mathbb{E}_{\boldsymbol{\Omega}}\,\mathbb{E}_{\boldsymbol{\Psi}}\,\|\boldsymbol{\Psi}_2^\dagger\boldsymbol{\Psi}_1(\boldsymbol{P}^*\boldsymbol{A})\|_{\mathrm{F}}^2\right)^{1/2} \\
&\le \sqrt{1 + f(r,k)}\cdot\|\boldsymbol{A} - [\![\boldsymbol{A}]\!]_r\|_{\mathrm{F}} + 2\sqrt{f(k,\ell)}\cdot\left(\mathbb{E}_{\boldsymbol{\Omega}}\,\|\boldsymbol{A} - \boldsymbol{Q}\boldsymbol{Q}^*\boldsymbol{A}\|_{\mathrm{F}}^2\right)^{1/2} \\
&\le \left[\sqrt{1 + f(r,k)} + 2\sqrt{f(k,\ell)(1 + f(r,k))}\right]\cdot\|\boldsymbol{A} - [\![\boldsymbol{A}]\!]_r\|_{\mathrm{F}}.
\end{aligned}$$

The first relation follows from Jensen's inequality. We invoke Proposition 9.2 to bound the first term, and we use Lemma 8.7 to compute the expectation of the second term. Last, we invoke Fact 8.3. This is the required estimate.

10. Computational Experiments. This section presents the results of some numerical tests designed to evaluate the empirical performance of our low-rank reconstruction algorithms. We also offer empirical comparisons with the method proposed by Woodruff [25, Thm. 4.3].

In these experiments, we consider several classes of synthetic matrices that admit accurate low-rank approximations, and we also study a specific matrix drawn from an application in large-scale optimization. The figures map the topography of the approximation error as a function of the sketch size parameters k and ℓ. Using both theory and experimental data, we investigate methods for selecting k and ℓ optimally when the total sketch size $k + \ell$ is fixed. We also verify that the error bound from Theorem 4.1 is sharp for one class of examples.

10.1. Three Classes of Input Matrices. To begin, let us describe three types of (complex-valued) input matrices that we use to investigate the empirical performance of our low-rank reconstruction algorithms. Figure 10.1 illustrates the singular spectrum of a matrix from each of the categories.

10.1.1. A Low-Rank Matrix Plus White Noise. Select a dimension parameter n and a target rank r. We consider matrices of the form

$$\boldsymbol{A}_{\mathrm{lr}} \quad := \quad \begin{bmatrix} \mathbf{I}_r & \mathbf{0} \\ \mathbf{0} & \mathbf{0} \end{bmatrix} \quad + \quad \sqrt{\gamma r n^{-2}}\boldsymbol{G} \quad \in \quad \mathbb{C}^{n\times n}.$$

Here, $\mathbf{I}_r$ denotes the $r \times r$ identity matrix. The parameter γ controls the Frobenius norm of the noise, and $\boldsymbol{G}$ is a (complex) standard normal matrix.

In our numerical work, we set the matrix dimension $n = 10^4$ and the rank parameter $r = 5$. We fix the noise level $\gamma = 10^{-3}$. The results are qualitatively similar for γ in the range 10^{-2} to 10^{-8}. Note that the experiments for this model are performed on a fixed matrix drawn from this class.

10.1.2. A Matrix Whose Spectrum Has Polynomial Decay. Select a dimension parameter n. We construct matrices of the form

$$\boldsymbol{A}_{\mathrm{decay}} \quad := \quad \operatorname{diag}(1^{-p}, 2^{-p}, 3^{-p}, \dots, n^{-p}) \quad \in \quad \mathbb{C}^{n\times n},$$

where $p > 0$ is a parameter that controls the polynomial rate of decay.

In our numerical work, the matrix dimension $n = 10^4$, and we consider decay parameters $p = 1$ and $p = 2$. We fix the target rank $r = 5$.

10.1.3. A Matrix from an Application in Optimization. Last, we consider a complex psd matrix obtained from an application:

$$\boldsymbol{A}_{\mathrm{appl}} \quad \in \quad \mathbb{H}_+^n(\mathbb{C}) \quad \text{with} \quad n = 25,921.$$

The first five singular values of $\boldsymbol{A}_{\mathrm{appl}}$ decrease from 1 to around 0.1; there is a significant gap between the fifth and sixth singular value; the remaining nonzero singular values decay very rapidly; the matrix has rank 250. See Figure 10.1.

The matrix $\boldsymbol{A}_{\mathrm{appl}}$ arises from an algorithm for solving a large-scale real-world phase retrieval problem. See our paper [6] for more details about the role of single-view low-rank approximation in this context. The phase retrieval application requires us to produce a psd approximation of the matrix $\boldsymbol{A}_{\mathrm{appl}}$ with target rank $r = 1$. For completeness, we also explore the behavior of unstructured approximations, as well as approximations with target rank $r = 5$.

10.1.4. Remarks. We have chosen to focus on the case where the input matrix is square ($m = n$) to reduce the number of moving parts. The sketching methods developed in this paper use standard normal test matrices, so the sketches and the algorithms are invariant under changes of coordinates (in exact arithmetic). As a consequence, we have built our synthetic examples around nonnegative, diagonal matrices. The matrix $\boldsymbol{A}_{\mathrm{appl}}$ from the phase retrieval problem is not diagonal.

10.2. Overview of Experimental Setup. For our numerical assessment, we work over the complex field $\mathbb{F} = \mathbb{C}$. Results for the real field $\mathbb{F} = \mathbb{R}$ are similar.

Let us summarize the procedure for studying the behavior of a specified reconstruction method on a given input matrix. Fix the input matrix $\boldsymbol{A}$ and the target rank r. Then select a pair (k, ℓ) of sketch size parameters where $k \geq r$ and $\ell \geq r$.

Each trial has the following form. We draw (complex) standard normal test matrices $(\boldsymbol{\Omega}, \boldsymbol{\Psi})$ to form the sketch $(\boldsymbol{Y}, \boldsymbol{W})$ of the input matrix. We compute an approximation $\hat{\boldsymbol{A}}_{\mathrm{out}}$ of the matrix $\boldsymbol{A}$ by means of a specified reconstruction algorithm. Then we calculate the error relative to the best rank-r approximation:

$$\text{relative error} \quad := \quad \frac{\|\boldsymbol{A} - \hat{\boldsymbol{A}}_{\mathrm{out}}\|_{\mathrm{F}}}{\|\boldsymbol{A} - [\![\boldsymbol{A}]\!]_r\|_{\mathrm{F}}} - 1. \tag{10.1}$$

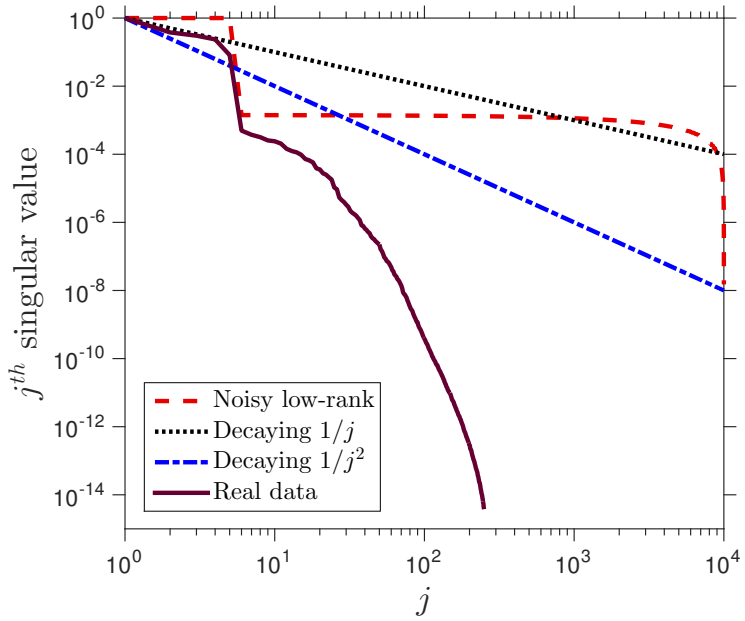

FIG. 10.1: For each of four matrices, this plot displays the singular value spectrum. The solid black curve is the spectrum of the matrix $\boldsymbol{A}_{\text{appl}}$ from a phase retrieval problem. The noisy low-rank matrix $\boldsymbol{A}_{\text{lr}}$ and the matrices $\boldsymbol{A}_{\text{decay}}$ with decaying spectrum are synthetic.

If $\hat{\boldsymbol{A}}_{\text{out}}$ is a rank-r approximation of $\boldsymbol{A}$, the relative error is always nonnegative.

To obtain each data point, we repeat the procedure from the last paragraph 50 times, each time with the same input matrix $\boldsymbol{A}$ and an independent draw of the test matrices $(\boldsymbol{\Omega}, \boldsymbol{\Psi})$. Then we report the average relative error over the 50 trials.

We include our MATLAB implementations in the supplementary materials for readers who seek more details on the methodology.

10.3. Theory versus Practice. Our first experiment is designed to assess the accuracy of Theorem 4.1, the theoretical error bound for Algorithm 4, which produces a rank-k approximation $\hat{\boldsymbol{A}}$ of an input matrix $\boldsymbol{A}$. For reference, the bound reads

$$\mathbb{E}\,\|\boldsymbol{A} - \hat{\boldsymbol{A}}\|_{\text{F}}^2 \le (1 + f(r,k))(1 + f(k,\ell)) \cdot \|\boldsymbol{A} - [\![\boldsymbol{A}]\!]_r\|_{\text{F}}^2. \tag{10.2}$$

The function f is defined in (4.5).

For this experiment, we draw the input matrix $\boldsymbol{A}$ according to the noisy low-rank model $\boldsymbol{A}_{\text{lr}}$, as discussed in subsection 10.1.1. We set the target rank $r = 5$, and we sweep through a subset of the sketch size parameters $k = 1, \dots, 150$ and $\ell = k, \dots, 600$. We chart the quality of the reconstructions obtained from Algorithm 4 and the error bound (10.2). See Figure 10.2 for the results.

We discover that the theoretical bound (10.2) closely tracks the error in the rank-k reconstruction $\hat{\boldsymbol{A}}$ from Algorithm 4. In other words, for the noisy low-rank model, the theoretical error bound is empirically sharp! As a consequence, we may use the right-hand side of (10.2) as a proxy for the error achieved by Algorithm 4.

10.4. Exploring the Parameter Space. Next, we survey how the fixed-rank reconstruction method, Algorithm 5, behaves for input matrices from each of the three

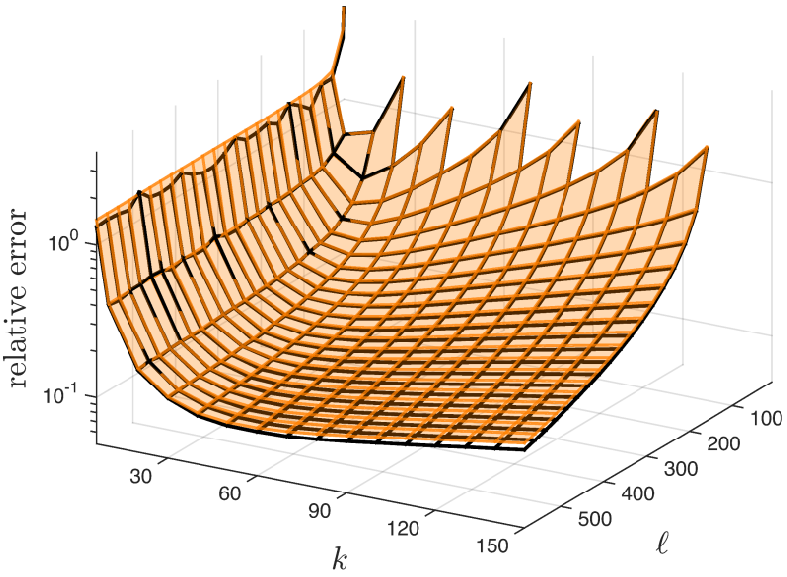

FIG. 10.2: This plot compares the error from Algorithm 4 (black mesh) with the theoretical bound (10.2) (orange shaded surface) for the noisy low-rank matrix model.

classes as we vary the sketch size parameters (k, ℓ). We include comparisons with our formulation (5.6) of Woodruff's fixed-rank reconstruction [25, Thm. 4.3].

First, let us consider the noisy low-rank matrix $\boldsymbol{A}_{\mathrm{lr}}$, discussed in subsection 10.1.1. Figure 10.3a shows that Algorithm 5 and Woodruff's method (5.6) have very similar behavior at the target rank $r = 5$. Observe that Woodruff's method may behave substantially better than ours when ℓ is very close to k. In fact, these parameter choices are not appropriate for our methods because we can always reduce the value of k to improve the performance of Algorithm 5.

Second, we look at matrices $\boldsymbol{A}_{\mathrm{decay}}$ with polynomially decaying singular values, as discussed in subsection 10.1.2. Recall that the target rank $r = 5$. Figures 10.3b and 10.3c compare the behavior of the reconstruction algorithms for decay exponents $p = 1$ and $p = 2$. When $p = 1$, Algorithm 5 and Woodruff's formula (5.6) perform similarly. As the decay rate p increases, Algorithm 5 offers increasing benefits over Woodruff's technique.

Last, we examine the matrix $\boldsymbol{A}_{\mathrm{appl}}$ derived from the phase retrieval application. Figures 10.3d and 10.3e display reconstruction errors at target rank $r = 1$ and $r = 5$. In addition to the unstructured fixed-rank approximations, we also study the performance of Algorithm 9, which enforces the psd constraint. The psd reconstruction is uniformly superior, with the unstructured approximation from Algorithm 5 close behind. Woodruff's approach (5.6) is typically worse by orders of magnitude.

10.5. Selecting the Best Sketch Size Parameters. Our primary goal is to obtain the best possible fixed-rank reconstruction of an input matrix using the smallest sketch possible. For standard normal test matrices, the storage cost of the sketch is directly proportional to the sum $k + \ell$ of the sketch size parameters. In this section, we investigate the best way to apportion k and ℓ when we fix the sketch size $k + \ell$

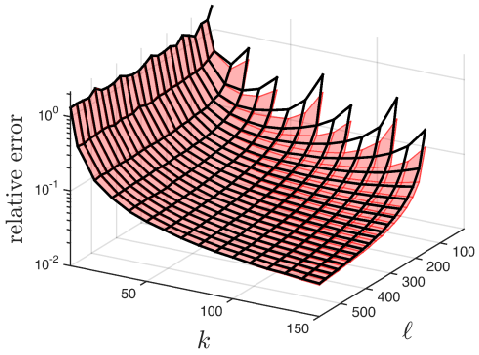

(A) Algorithm 5 (black mesh) versus Woodruff's method (red shaded surface) for reconstructing a noisy low-rank matrix $\boldsymbol{A}_{\mathrm{lr}}$.

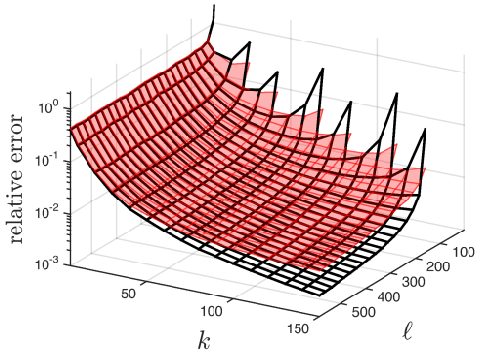

(B) Algorithm 5 (black mesh) versus Woodruff's method (red surface) for a matrix $\boldsymbol{A}_{\mathrm{decay}}$ with singular values $\sigma_j = 1/j$.

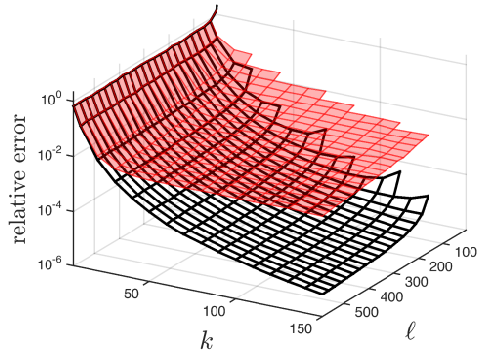

(C) Algorithm 5 (black mesh) versus Woodruff's method (red surface) for a matrix $\boldsymbol{A}_{\mathrm{decay}}$ with singular values $\sigma_j = 1/j^2$.

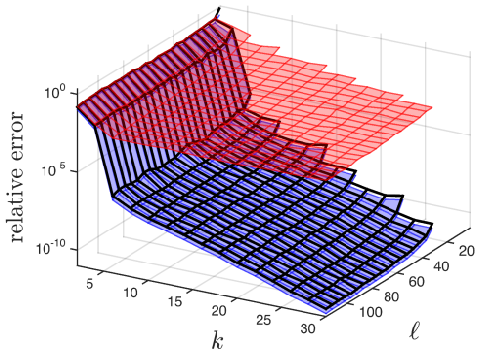

(D) Algorithm 9 (blue shaded surface) versus Algorithm 5 (black mesh) and Woodruff's method (red surface) for a matrix $\boldsymbol{A}_{\mathrm{appl}}$ from a phase retrieval application. ($r = 1$).

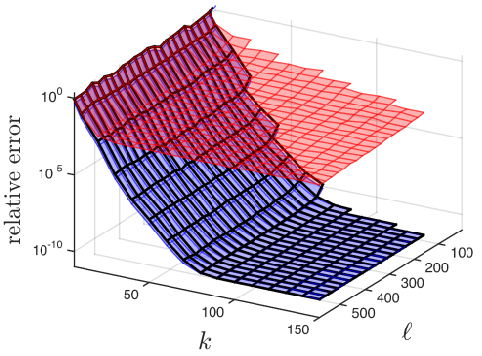

(E) Algorithm 9 (blue surface) versus Algorithm 5 (black mesh) and Woodruff's method (red surface) for a matrix $\boldsymbol{A}_{\mathrm{appl}}$ from a phase retrieval application. ($r = 5$).

FIG. 10.3: The panels display the empirical performance of Algorithms 5 and 9 as compared to our formulation (5.6) of Woodruff's fixed-rank reconstruction [25, Thm. 4.3]. Matrix dimensions are $m = n = 10^4$ for synthetic examples and $m = n = 25,921$ for the phase retrieval matrix. The target rank $r = 5$, unless noted. The sketch size parameters (k, ℓ) are variables. Relative error is defined in (10.1).

and the target rank r.

First, we develop a theory-driven approach for selecting the sketch size parameters. In subsection 10.3, we observed that the theoretical bound (10.2) accurately models the error in the low-rank reconstruction from Algorithm 4 for one class of input matrices. Therefore, an appealing way to pick sketch size parameters (k, ℓ) is to minimize the bound (10.2) with the sum $k + \ell$ fixed, subject to the constraints $k > r + \alpha$ and $\ell > k + \alpha$.

To that end, introduce notation $T := k + \ell$ for the total sketch size, and assume that $T > 2r$. For $\mathbb{F} = \mathbb{C}$, the approach in the last paragraph leads to the "theoretically optimal" sketch size parameters

$$k_\star := \left\lfloor T \cdot \frac{\sqrt{r(T-r)} - r}{T - 2r} \right\rfloor \quad \text{and} \quad \ell_\star := T - k_\star. \tag{10.3}$$

We omit the routine details behind this calculation.

Second, we would like to understand how perfectly tuned variants of the algorithms compare with each other at a given sketch size. To do so, we can use the data from the experiments in subsection 10.4 to minimize the empirical reconstruction error for each algorithm over pairs (k, ℓ) with the sum $k + \ell$ fixed. The best possible choice of (k, ℓ) for a given method is referred to as the *oracle sketch size*. In practice, we cannot identify the oracle sketch size *a priori*, although numerical studies may provide some insight.

Figure 10.4 displays the performance of several reconstruction methods for three classes of input matrices, as a function of the sum $k + \ell$. For each algorithm, we plot the empirical error attained when the sketch size parameters are chosen according to (10.3). We also plot the empirical error that the algorithm achieves for the oracle sketch size parameters.

For all three classes of matrix, the performance of Algorithms 5 and 9 matches or exceeds the performance of Woodruff's method (5.6). This is true both for the theoretically motivated choice and the oracle choice of the sketch size parameters. When the input matrix has decaying singular values, our methods can achieve reconstruction errors orders of magnitude better than Woodruff's. For the matrix $\boldsymbol{A}_{\text{appl}}$ from the phase retrieval application, the advantages of our method are undeniable.

10.6. Conclusions. This paper develops a collection of low-rank matrix reconstruction algorithms that only require a single view of the matrix. Our empirical studies demonstrate that these methods are effective for several types of matrices that admit low-rank approximations. Our theoretical analysis provides practical guidance for selecting sketch size parameters to minimize the total storage cost of the sketch. Moreover, our methods compare favorably with the numerical formulation (5.6) of the single-view reconstruction method proposed by Woodruff [25, Thm. 4.3].

For a given input matrix, the quality of a single-view low-rank reconstruction depends on the singular value spectrum. For a low-rank matrix contaminated with white noise, Woodruff's approach is slightly better than ours. When the spectrum of the matrix decays polynomially, our method outperforms Woodruff's approach, sometimes dramatically. Our method is markedly superior for a matrix derived from a phase retrieval application. In addition, our method can achieve very small relative errors, while experience suggests that Woodruff's method does not offer this benefit.

In conclusion, the empirical evidence supports the claim that our algorithms provide a valuable suite of tools for low-rank matrix approximation from a single view.

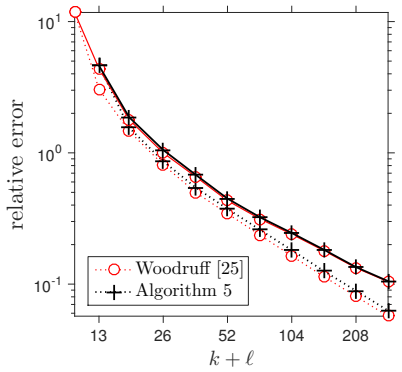

(A) Noisy low-rank matrix $\boldsymbol{A}_{\mathrm{lr}}$

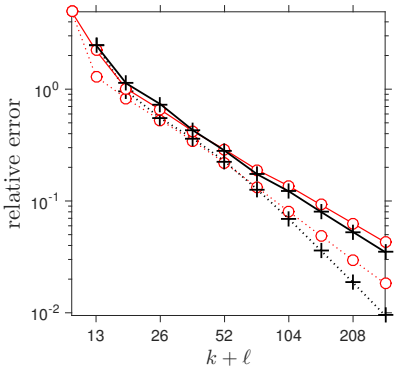

(B) Matrix $\boldsymbol{A}_{\mathrm{decay}}$ with $\sigma_j = 1/j$

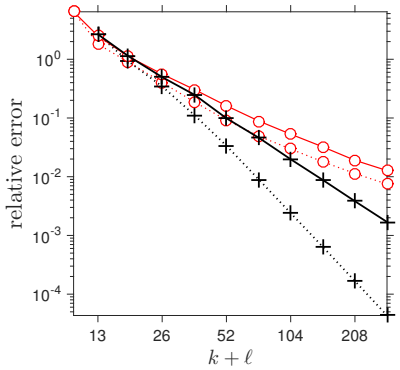

(C) Matrix $\boldsymbol{A}_{\mathrm{decay}}$ with $\sigma_j = 1/j^2$

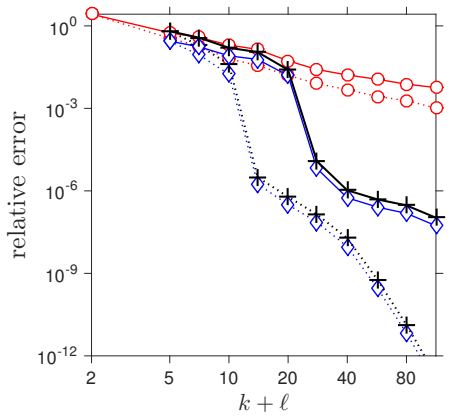

(D) Phase retrieval matrix $\boldsymbol{A}_{\mathrm{appl}}$ $(r = 1)$

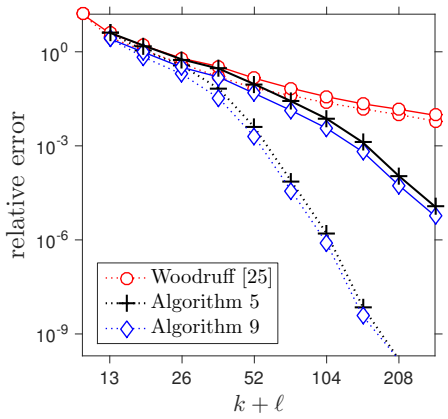

(E) Phase retrieval matrix $\boldsymbol{A}_{\mathrm{appl}}$ $(r = 5)$

FIG. 10.4: The panels display the empirical performance of Algorithms 5 and 9 as compared to our formulation (5.6) of Woodruff's fixed-rank reconstruction. Matrix dimensions are $m = n = 10^4$ for synthetic examples and $m = n = 25,921$ for the phase retrieval matrix. The target rank $r = 5$, unless otherwise stated. The variable is the sum $k + \ell$ of the sketch size parameters. **Solid lines** present the error at the pair $(k_\star, \ell_\star)$ defined in (10.3). **Dashed lines** reflect the minimum empirical error attained for any (k, ℓ). Relative error is defined in (10.1).

Acknowledgments. The authors would like to thank Gunnar Martinsson and Mark Tygert for helpful conversations.

REFERENCES

[1] N. Ailon and B. Chazelle, *Approximate nearest neighbors and the fast Johnson-Lindenstrauss transform*, in STOC'06: Proceedings of the 38th Annual ACM Symposium on Theory of Computing, ACM, New York, 2006, pp. 557–563, doi:10.1145/1132516.1132597, http://dx.doi.org/10.1145/1132516.1132597.

[2] N. Ailon and B. Chazelle, *The fast Johnson-Lindenstrauss transform and approximate nearest neighbors*, SIAM J. Comput., 39 (2009), pp. 302–322, doi:10.1137/060673096, http://dx.doi.org/10.1137/060673096.

[3] J. Bourgain, S. Dirksen, and J. Nelson, *Toward a unified theory of sparse dimensionality reduction in Euclidean space*, Geom. Funct. Anal., 25 (2015), pp. 1009–1088, doi:10.1007/s00039-015-0332-9, http://dx.doi.org/10.1007/s00039-015-0332-9.

[4] C. Boutsidis and A. Gittens, *Improved matrix algorithms via the subsampled randomized Hadamard transform*, SIAM J. Matrix Anal. Appl., 34 (2013), pp. 1301–1340, doi:10.1137/120874540, http://dx.doi.org/10.1137/120874540.

[5] S. Boyd and L. Vandenberghe, *Convex optimization*, Cambridge University Press, Cambridge, 2004, doi:10.1017/CBO9780511804441, http://dx.doi.org/10.1017/CBO9780511804441.

[6] V. Cevher, J. A. Tropp, M. Udell, and A. Yurtsever, *Sketchy decisions: convex optimization with optimal storage*, May 2016, arXiv:1608.xxxxx [math.NA]. Manuscript.

[7] K. L. Clarkson and D. P. Woodruff, *Numerical linear algebra in the streaming model*, in Proc. 41st ACM Symposium on Theory of Computing (STOC), Bethesda, 2009.

[8] K. L. Clarkson and D. P. Woodruff, *Low rank approximation and regression in input sparsity time*, in STOC'13—Proceedings of the 2013 ACM Symposium on Theory of Computing, ACM, New York, 2013, pp. 81–90, doi:10.1145/2488608.2488620, http://dx.doi.org/10.1145/2488608.2488620.

[9] M. Cohen, *Nearly tight oblivious subspace embeddings by trace inequalities*, in Proc. 27th Ann. ACM-SIAM Symp. Discrete Algorithms (SODA), Arlington, Jan. 2016, pp. 278–287.

[10] J. Demmel, I. Dumitriu, and O. Holtz, *Fast linear algebra is stable*, Numer. Math., 108 (2007), pp. 59–91, doi:10.1007/s00211-007-0114-x, http://dx.doi.org/10.1007/s00211-007-0114-x.

[11] P. Drineas, R. Kannan, and M. W. Mahoney, *Fast Monte Carlo algorithms for matrices. II. Computing a low-rank approximation to a matrix*, SIAM J. Comput., 36 (2006), pp. 158–183, doi:10.1137/S0097539704442696, http://dx.doi.org/10.1137/S0097539704442696.

[12] A. Frieze, R. Kannan, and S. Vempala, *Fast Monte-Carlo algorithms for finding low-rank approximations*, J. ACM, 51 (2004), pp. 1025–1041, doi:10.1145/1039488.1039494, http://dx.doi.org/10.1145/1039488.1039494.

[13] M. Gu, *Subspace iteration randomization and singular value problems*, SIAM J. Sci. Comput., 37 (2015), pp. A1139–A1173, doi:10.1137/130938700, http://dx.doi.org/10.1137/130938700.

[14] N. Halko, P. G. Martinsson, and J. A. Tropp, *Finding structure with randomness: probabilistic algorithms for constructing approximate matrix decompositions*, SIAM Rev., 53 (2011), pp. 217–288.

[15] N. J. Higham, *Matrix nearness problems and applications*, in Applications of matrix theory (Bradford, 1988), Oxford Univ. Press, New York, 1989, pp. 1–27.

[16] M. W. Mahoney, *Randomized algorithms for matrices and data*, Foundations and Trends® in Machine Learning, 3 (2011), pp. 123–224.

[17] P.-G. Martinsson, V. Rokhlin, and M. Tygert, *A randomized algorithm for the decomposition of matrices*, Appl. Comput. Harmon. Anal., 30 (2011), pp. 47–68, doi:10.1016/j.acha.2010.02.003, http://dx.doi.org/10.1016/j.acha.2010.02.003.

[18] X. Meng and M. W. Mahoney, *Low-distortion subspace embeddings in input-sparsity time and applications to robust linear regression*, in STOC'13—Proceedings of the 2013 ACM Symposium on Theory of Computing, ACM, New York, 2013, pp. 91–100, doi:10.1145/2488608.2488621, http://dx.doi.org/10.1145/2488608.2488621.

[19] S. Muthukrishnan, *Data streams: algorithms and applications*, Found. Trends Theor. Comput. Sci., 1 (2005), pp. 117–236.

[20] J. Nelson and H. L. Nguyen, *OSNAP: faster numerical linear algebra algorithms via sparser subspace embeddings*, in 2013 IEEE 54th Annual Symposium on Foundations of Com-

puter Science—FOCS 2013, IEEE Computer Soc., Los Alamitos, CA, 2013, pp. 117–126, doi:10.1109/FOCS.2013.21, http://dx.doi.org/10.1109/FOCS.2013.21.

[21] J. Nelson and H. L. Nguyen, *Lower bounds for oblivious subspace embeddings*, in Automata, languages, and programming. Part I, vol. 8572 of Lecture Notes in Comput. Sci., Springer, Heidelberg, 2014, pp. 883–894, doi:10.1007/978-3-662-43948-7_73, http://dx.doi.org/10.1007/978-3-662-43948-7_73.

[22] C. H. Papadimitriou, P. Raghavan, H. Tamaki, and S. Vempala, *Latent semantic indexing: a probabilistic analysis*, J. Comput. System Sci., 61 (2000), pp. 217–235, doi:10.1006/jcss.2000.1711, http://dx.doi.org/10.1006/jcss.2000.1711. Special issue on the Seventeenth ACM SIGACT-SIGMOD-SIGART Symposium on Principles of Database Systems (Seattle, WA, 1998).

[23] T. Sarlós, *Improved approximation algorithms for large matrices via random projections*, in Proc. 47th Ann. IEEE Symposium on Foundations of Computer Science (FOCS), Berkeley, 2006.

[24] J. A. Tropp, *Improved analysis of the subsampled randomized Hadamard transform*, Adv. Adapt. Data Anal., 3 (2011), pp. 115–126, doi:10.1142/S1793536911000787, http://dx.doi.org/10.1142/S1793536911000787.

[25] D. P. Woodruff, *Sketching as a tool for numerical linear algebra*, Found. Trends Theor. Comput. Sci., 10 (2014), pp. iv+157.

[26] F. Woolfe, E. Liberty, V. Rokhlin, and M. Tygert, *A fast randomized algorithm for the approximation of matrices*, Appl. Comput. Harmon. Anal., 25 (2008), pp. 335–366.